FIBROSIS

Hexokinase 2 couples glycolysis with the profibrotic actions of TGF-β

Xueqian Yin*, Malay Choudhury, Jeong-Han Kang†, Kyle J. Schaefbauer, Mi-Yeon Jung‡, Mahefatiana Andrianifahanana, Danielle M. Hernandez§, Edward B. Leof||

Metabolic dysregulation in fibroblasts is implicated in the profibrotic actions of transforming growth factor–β (TGF-β). Here, we present evidence that hexokinase 2 (HK2) is important for mediating the fibroproliferative activity of TGF-β both in vitro and in vivo. Both Smad-dependent and Smad-independent TGF-β signaling induced HK2 accumulation in murine and human lung fibroblasts through induction of the transcription factor c-Myc. Knockdown of HK2 or pharmacological inhibition of HK2 activity with Lonidamine decreased TGF-β–stimulated fibrogenic processes, including profibrotic gene expression, cell migration, colony formation, and activation of the transcription factors YAP and TAZ, with no apparent effect on cellular viability. Fibroblasts from patients with idiopathic pulmonary fibrosis (IPF) exhibited an increased abundance of HK2. In a mouse model of bleomycin-induced lung fibrosis, Lonidamine reduced the expression of genes encoding profibrotic markers (*collagen*Iα*1*, *EDA-fibronectin*, α *smooth muscle actin*, and *connective tissue growth factor*) and stabilized or improved lung function as assessed by measurement of peripheral blood oxygenation. These findings provide evidence of how metabolic dysregulation through HK2 can be integrated within the context of profibrotic TGF-β signaling.

INTRODUCTION

Fibroproliferative disorders encompass a wide variety of diseases that affect essentially all organs (*1*–*4*). Because treatment options are often ineffective and/or unavailable, these diseases have been estimated to be responsible for upward of 45% of all deaths in the developed world (*5*–*7*). Moreover, although our understanding of the molecular and cellular changes associated with these disorders has increased (*4*, *8*, *9*), this has not resulted in effective clinical outcomes for the vast majority of patients (*10*–*13*).

The primary cytokine responsible for the initiation and/or progression of tissue and organ fibrosis is transforming growth factor–β (TGF-β), which both directly stimulates profibrotic responses and induces additional mediators such as platelet-derived growth factor (PDGF) (*14*), Erb-B receptor ligands (*15*), and connective tissue growth factor (CTGF) (*16*). TGF-β is a 25-kDa polypeptide that can either stimulate or inhibit various cellular processes (*17*, *18*). The type I, type II, and type III (betaglycan) receptors are the primary cell surface receptors for TGF-β (*19*). The type I and type II TGF-β receptors (TβRI and TβRII, respectively) are single-pass, transmembrane serine-threonine kinases (*20*, *21*). Ligand binding to the constitutively phosphorylated TβRII results in TβRI recruitment and transphosphorylation by TβRII, resulting in activation of a heteromeric TGFβR complex (*22*, *23*). Subsequent intracellular signaling is primarily mediated by the Smad proteins, Smad2 and Smad3 (Smad2/3). These cytoplasmic 42- to 60-kDa proteins form hetero-oligomeric complexes with Smad4 after receptor activation and translocate to the nucleus where they regulate gene transcription (*24*, *25*). Although the Smads are implicated in mediating many aspects of TGF-β family member activity, work by us and others has shown non-Smad signaling to be critical for a subset of TGF-β responses (*18*, *26*–*28*).

Although both Smad and non-Smad pathways are known to affect profibrotic TGF-β signaling, how they interface with other aspects of TGF-β action, such as the regulation of cellular metabolism, is relatively unexplored. A role for altered metabolism has been extensively investigated in neoplastic diseases (*29*, *30*), but analogous reports in fibroproliferative disorders are relatively limited (*31*–*34*). To that end, we previously reported a requirement for the induction of the glucose transporter GLUT1 in TGF-β–driven fibrogenic processes (*35*), and another publication further defined this association by integrating it within the serine-glycine biosynthetic pathway to meet the demands for increased collagen synthesis during myofibroblast differentiation (*36*). In the current study, we extend this interrelation of glucose uptake, glycolysis, and profibrotic TGF-β action by documenting a role for hexokinase 2 (HK2), both in vitro and in vivo. In that HK2 and GLUT1 are both stimulated by TGF-β, this previously unknown relationship has implications for several homeostatic and/or pathologic cellular processes.

HKs catalyze the first obligatory step in glucose metabolism to generate glucose-6-phosphate (*37*). This not only furthers glucose entry by maintaining the concentration gradient for facilitated glucose influx but also provides the first intermediate for essentially all major pathways using glucose. There are four HK isoforms in mammalian tissues: HK1, HK2, HK3, and HK4. Although each of these isoforms has distinct roles, the production or activity of HK2 is increased in many tumor types and plays a central role in growth factor–mediated cell survival (*38*–*40*).

In the current study, we investigated profibrotic TGF-β signaling in mouse and human lung fibroblasts and in a murine in vivo model of lung fibrosis. We found that TGF-β induced HK2 accumulation in fibroblasts through Smad2/3 and c-Myc, and this was necessary for the TGF-β–stimulated expression of profibrotic genes, cell migration, and colony formation in soft agar. TGF-β–mediated activation of the transcription factors YAP and TAZ (YAP/TAZ) was also attenuated

Thoracic Disease Research Unit, Division of Pulmonary and Critical Care Medicine, Department of Biochemistry and Molecular Biology, Mayo Clinic College of Medicine, Rochester, MN 55905, USA.
*Present address: Department of Molecular Medicine, Mayo Clinic College of Medicine, Rochester, MN 55905, USA.
†Present address: Department of Lab Medicine and Pathology, Mayo Clinic College of Medicine, Rochester, MN 55905, USA.
‡Present address: Department of Neurosurgery, Mayo Clinic College of Medicine, Rochester, MN 55905, USA.
§Present address: Department of Neurosurgery, University of Minnesota Twin Cities, Minneapolis, MN 55455, USA.
||Corresponding author. Email: leof.edward@mayo.edu

in the absence of HK2. Furthermore, fibroblasts isolated from patients with idiopathic pulmonary fibrosis (IPF) had increased basal amounts of HK2 but not HK1. Last, treatment with the HK2 inhibitor Lonidamine decreased the expression of profibrotic genes and stabilized lung function in a mouse model of bleomycin (BLM)–induced lung fibrosis.

RESULTS

HK2 is induced by TGF-β and increased in IPF fibroblasts

Whereas the profibrotic activity of TGF-β has been extensively documented (*41*, *42*), how these responses interface with cellular metabolism is relatively underinvestigated (*31*–*34*). Having previously determined that inhibition of GLUT1 production or activity impairs fibrogenic processes in a TGF-β–dependent manner (*35*), we sought to identify the operative mechanism(s). Stimulation of AKR-2B murine fibroblasts with TGF-β increased the expression, abundance, and activity of HK2 (Fig. 1, A to C). This increase was specific for HK2, because TGF-β decreased the abundance of the other mitochondrial HK, HK1 (Fig. 1A). Given that HK2 is the most proximal mediator of glucose metabolism, we next determined, first, whether this effect of TGF-β occurred in other murine and human fibroblasts, and, second, whether HK2 abundance was constitutively increased in fibroblasts isolated from patients with IPF. Consistent with that observed in AKR-2B cells, TGF-β treatment increased HK2 abundance in another murine fibroblast line (Swiss3T3), human lung fibroblast lines [Institute for Medical Research-90 (IMR90), Medical Research Council cell strain 5 (MRC5), and Tokyo Institute of Gerontology-1 (TIG-1)], and primary normal human lung fibroblasts (Fig. 1D and fig. S1A) as well as mitochondrial association (*37*–*40*) in MRC5 cells (fig. S1, B and C). Moreover, when primary fibroblasts isolated from normal donors and patients with IPF were examined, there was a notable

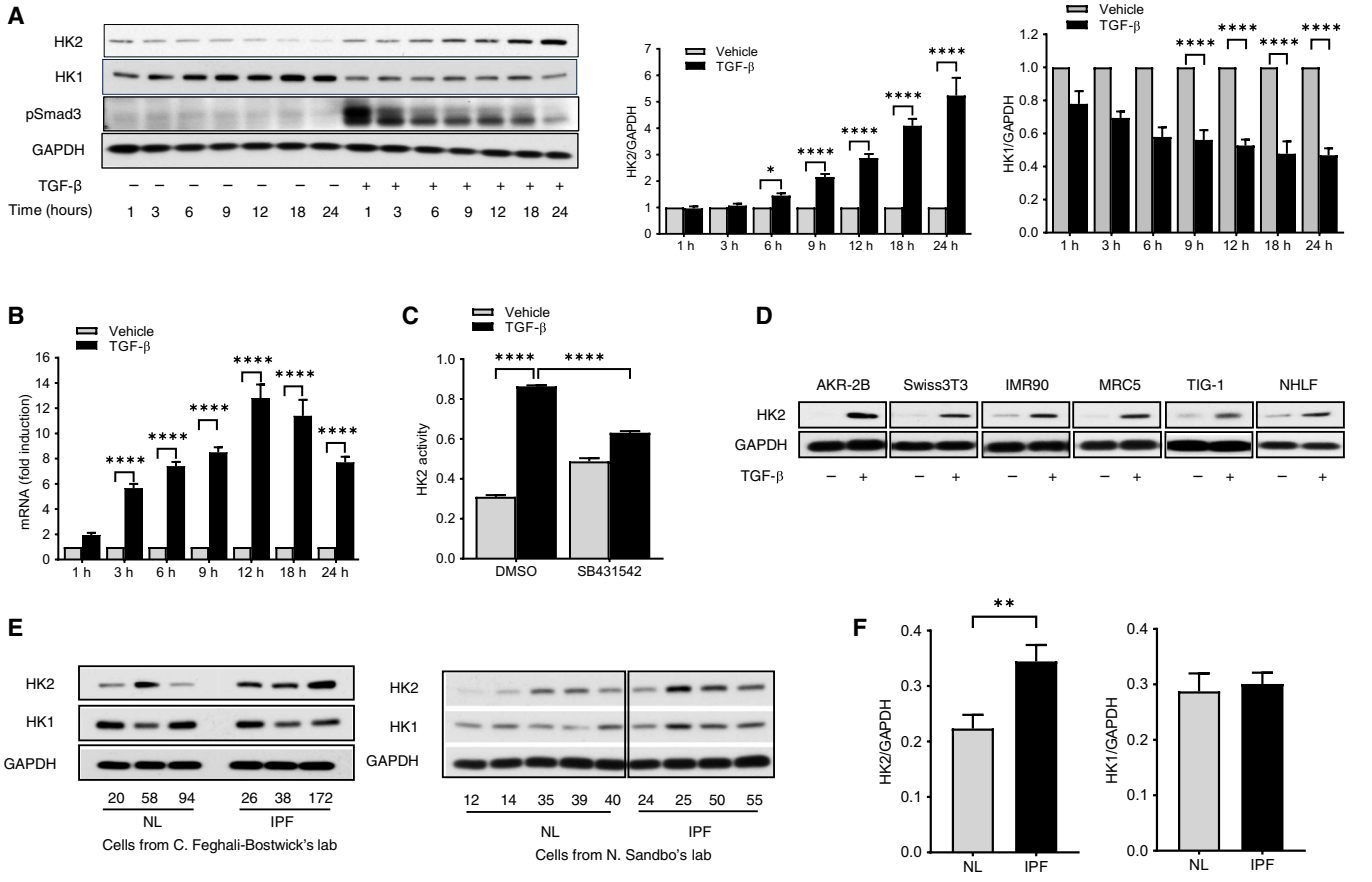

Fig. 1. TGF-β induces HK2 accumulation in murine and human fibroblasts. (**A**) Quiescent AKR-2B cells were treated with vehicle or TGF-β for the indicated amounts of time, and total protein was subjected to Western blot analysis for HK2, HK1, and phosphorylated Smad3 (pSmad3). Glyceraldehyde-3-phosphate dehydrogenase (GAPDH) is a loading control. Amounts of HK2 and HK1 relative to GAPDH were determined. $n = 3$ independent experiments. (**B**) AKR-2B cells were treated as in (A), and total RNA was subjected to real-time quantitative PCR using HK2 primers. *Smad4* was used as a normalization control. $n = 3$ independent experiments. (**C**) Quiescent AKR-2B cells were pretreated with vehicle or the TβRI inhibitor SB431542 for 1 hour and then stimulated with vehicle or TGF-β for 24 hours. HK2 protein was immunoprecipitated, and activity was determined relative to a purified HK standard. $n = 3$ independent experiments. (**D**) The indicated quiescent murine fibroblasts (AKR-2B and Swiss3T3), human lung fibroblast lines (IMR90, MRC5, and TIG-1), and primary normal human lung fibroblasts (NHLFs) were treated with vehicle (–) or TGF-β (+), and total proteins were immunoblotted for HK2. Blot is representative of three independent experiments. (**E**) Proliferating human normal lung (NL) fibroblast and idiopathic pulmonary fibrosis (IPF) fibroblast cells obtained from C. Feghali-Bostwick and N. Sandbo were lysed, and total proteins were immunoblotted for HK1 and HK2. Numbers indicate cell identifiers. (**F**) Relative abundances of HK2 and HK1 in NL and IPF cultures. Data reflect one experiment using patient lung samples from eight normal and seven IPF donors. All data reflect means ± SEM. Differences between groups were evaluated by unpaired Student's *t* test (F) or two-way ANOVA with Tukey post hoc analysis (A to C). $^{*}P < 0.05$, $^{**}P < 0.01$, $^{****}P < 0.0001$.

increase in HK2, but not in HK1, in the IPF samples (Fig. 1, E and F). These data are consistent with HK2 being both a downstream target and a potential mediator of TGF-β–dependent fibrogenic actions.

HK2 is required for profibrotic TGF-β signaling and YAP/TAZ activation

Because HK2 is known to have a fundamental role in various proliferative disorders (*38*, *43*), we initiated studies to assess the requirement for HK2 in the fibroproliferative actions of TGF-β after small interfering RNA (siRNA)–mediated HK2 knockdown. Loss of HK2 substantially decreased profibrotic TGF-β targets including collagen I (ColI), fibronectin (FN), α smooth muscle actin (αSMA), plasminogen activator inhibitor 1 (PAI-1), and CTGF in murine AKR-2B cells and human TIG-1 fibroblasts (Fig. 2, A and B, and fig. S2, A and B). Because the absence of HK2 activity prevents the oxidation of glucose to pyruvate, we tested whether exogenous pyruvate restored TGF-β–mediated induction of profibrotic markers. The addition of pyruvate overcame the inhibitory effect of HK2 knockdown on the induction of ColI, FN, αSMA, and CTGF by TGF-β (Fig. 2C and fig. S2C). HK2 knockdown also reduced TGF-β–stimulated cell migration (Fig. 2D) and colony formation in soft agar (Fig. 2E). This action of HK2 in profibrotic TGF-β signaling is downstream of canonical Smad or non-Smad activation, because loss of HK2 had no effect on the phosphorylation of Smad3 or Akt in response to TGF-β stimulation (fig. S3, A and B).

To confirm that these findings were not reflective of an off-target effect(s) of HK2 knockdown, analogous studies were performed using the mitochondrial HK inhibitor Lonidamine, which inhibits both HK1 and HK2 activities. Whereas Lonidamine decreased HK activity (fig. S4A), induction of TGF-β–stimulated fibroproliferative targets (Fig. 3, A to C, and fig. S5, A and B), cell migration (Fig. 3D), and growth in soft agar (Fig. 3E) in both murine and human fibroblasts, it had no biological effect on cell viability as assessed by the reduction of 3-[4,5-dimethylthiazole-2yl]-diphenyltetrazolium bromide (MTT)

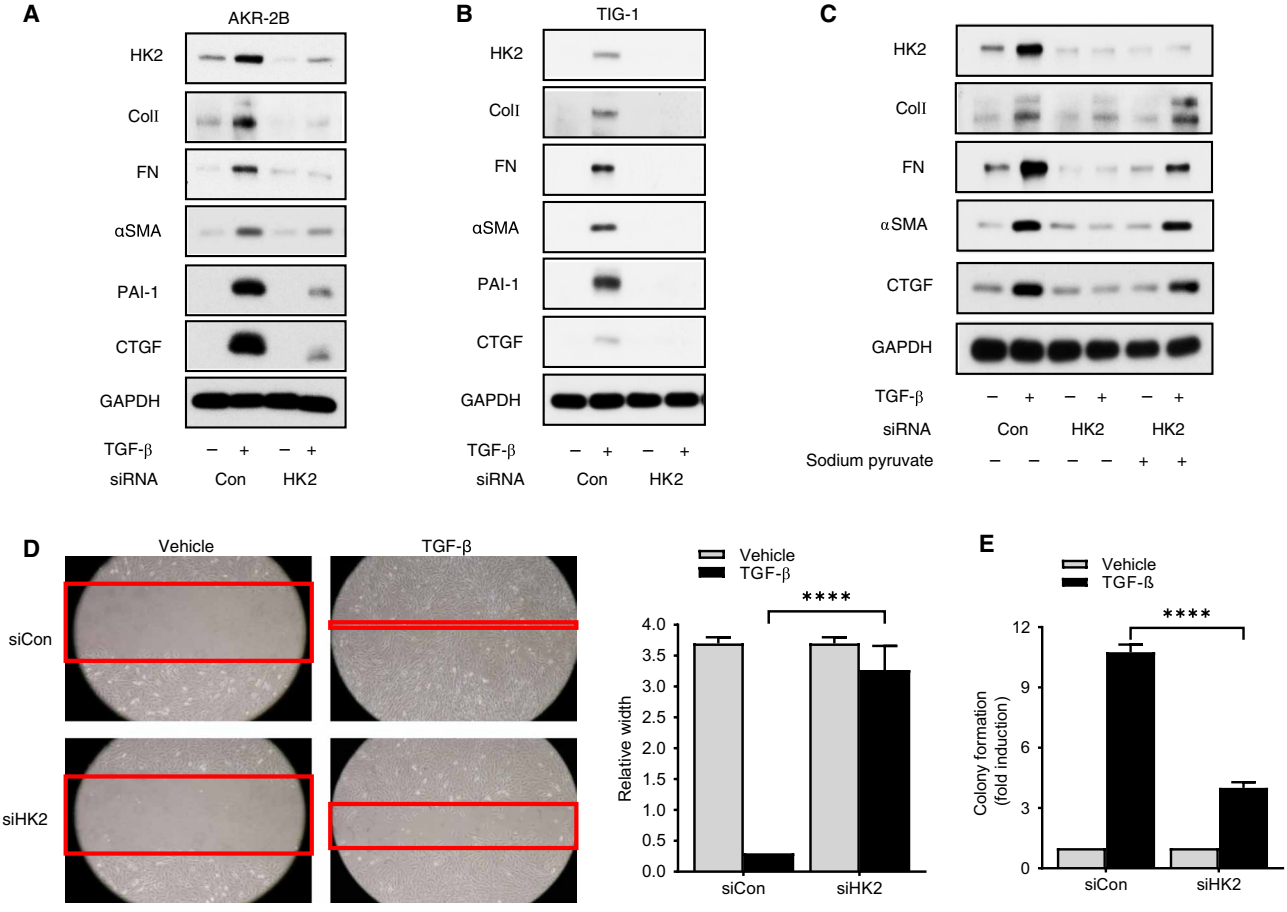

Fig. 2. Profibrotic TGF-β signaling depends on the induction of HK2. (**A**) AKR-2B cells were transiently transfected with control siRNA (siCon) or siRNA specific for HK2 (siHK2) and then stimulated with vehicle (–) or TGF-β (+). Western blotting on total cell proteins was performed for collagen I (ColI), fibronectin (FN), α smooth muscle actin (αSMA), plasminogen activator inhibitor (PAI-1), and connective tissue growth factor (CTGF). GAPDH is a loading control. Blot is representative of three independent experiments. (**B**) Human TIG-1 fibroblasts were treated and immunoblotted as in (A). Blot is representative of three independent experiments. (**C**) AKR-2B cells were transfected with control or HK2 siRNA, treated with vehicle or sodium pyruvate for 1 hour, and then stimulated with vehicle or TGF-β for 24 hours before Western blotting for the indicated proteins. Blot is representative of three independent experiments. (**D**) AKR-2B cells were transfected with control or HK2 siRNA and then subjected to scratch assays in the absence or presence of TGF-β and quantification of wound closure. Red lines indicate the leading edge after 24 hours. $n = 3$ independent experiments. (**E**) AKR-2B cells were transfected as in (A), and anchorage-independent growth in soft agar in the absence or presence of TGF-β was determined. $n = 3$ independent experiments with three technical replicates per condition. All data reflect the means ± SEM. Differences between groups were evaluated by two-way ANOVA with Tukey post hoc analysis. ****$P < 0.0001$.

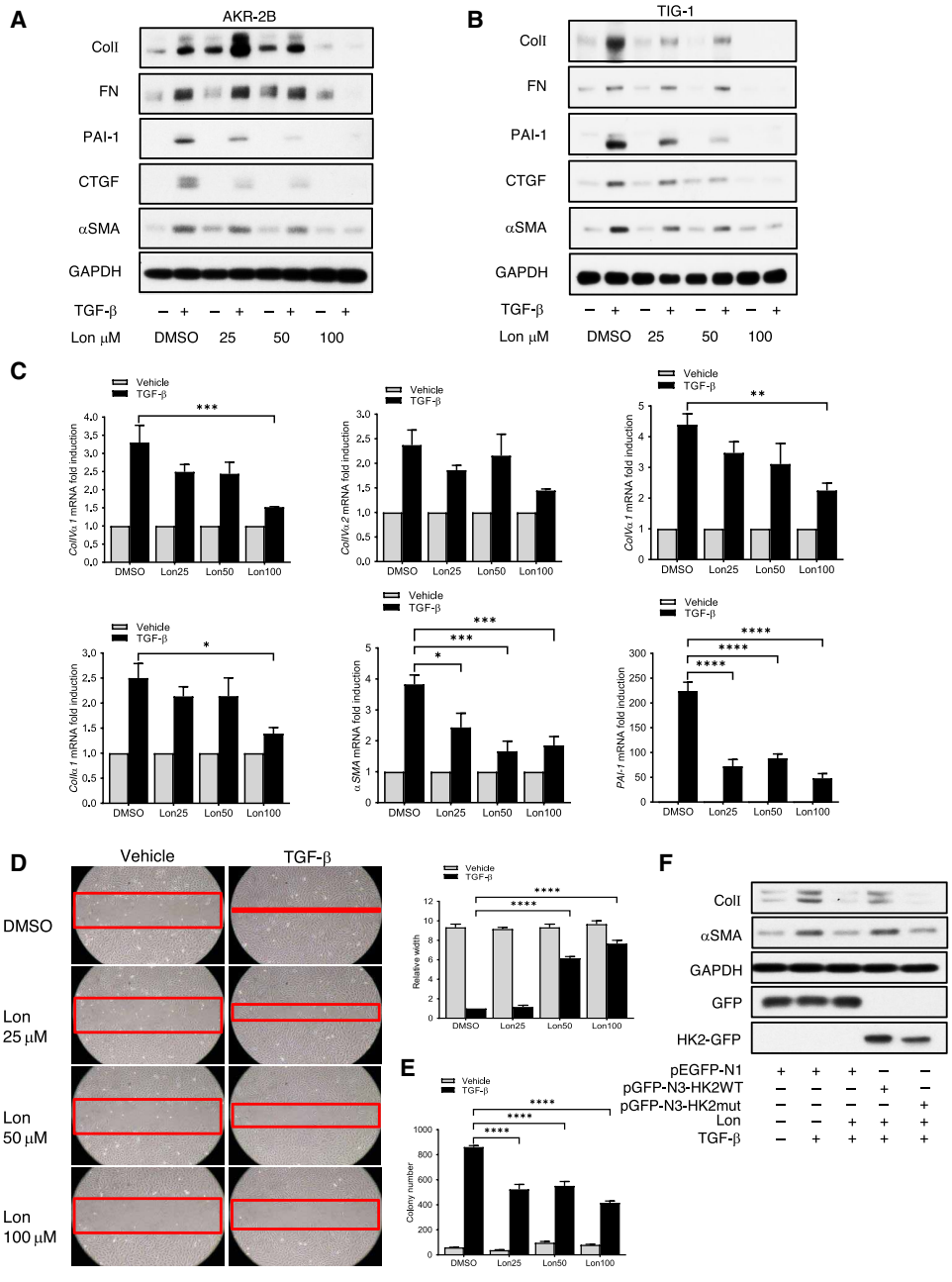

Fig. 3. HK2 activity is required for profibrotic TGF-β signaling. (**A**) Quiescent AKR-2B cells were treated with vehicle (DMSO) or Lonidamine (Lon) in the presence (+) or absence (–) of TGF-β. Western blotting was performed for ColI, FN, PAI-1, CTGF, and αSMA. GAPDH is a loading control. Data are representative of three independent experiments. (**B**) Quiescent human lung TIG-1 fibroblasts were treated and analyzed as in (A). Data are representative of three independent experiments. (**C**) Quiescent AKR-2B cells were treated for 12 hours with vehicle or Lonidamine in the presence or absence of TGF-β. Quantitative PCR was performed for the indicated transcripts. $n = 3$ independent experiments. (**D**) Scratch assays were performed on AKR-2B cells in the absence or presence of TGF-β and the indicated concentration of Lonidamine and then wound closure was quantified. Red lines indicate the leading edge after 24 hours. $n = 3$ independent experiments with three technical replicates per condition. (**E**) AKR-2B colony formation in soft agar in the presence or absence of TGF-β and the indicated Lonidamine concentrations was quantified. $n = 3$ independent experiments with three technical replicates per condition. (**F**) AKR-2B cells were transiently transfected with the indicated control (EGFP), kinase-active (HK2WT), or kinase-impaired (HK2mut) plasmids and then treated with vehicle or Lonidamine in the absence (–) or presence (+) of TGF-β before Western blotting for the indicated proteins. Data are representative of three independent experiments. Differences between groups were evaluated by two-way ANOVA with Tukey post hoc analysis. *$P < 0.05$, **$P < 0.01$, ***$P < 0.001$, ****$P < 0.0001$.

assay or cellular integrity (fig. S4, B and C). That these actions were reflective of Lonidamine's ability to inhibit HK2 kinase activity per se and not some kinase-independent role(s) were demonstrated by the ability of overexpression of wild-type HK2, but not kinase-dead HK2, to overcome the inhibitory response of Lonidamine on the accumulation of proteins encoded by TGF-β target genes (Fig. 3F and fig. S5C). Analogous to results observed with HK2 knockdown (fig. S3, A and B), TGF-β–stimulated Smad3 or Akt phosphorylation was unaffected by Lonidamine treatment (fig. S4, D and E). In addition to inhibiting HK activity, Lonidamine at higher concentrations also diminished the induction of HK2 protein yet had little to no effect on the TGF-β–induced decrease in HK1 (fig. S4F).

Increased abundance of HK2 would be expected to similarly increase both total cellular lactate and the oxygen consumption rate (OCR) under aerobic conditions (*31*–*34*). This was directly assessed in AKR-2B cells, TIG-1 cells, and primary human lung fibroblasts, where we determined that although TGF-β increased lactate production, inhibition of HK2 with Lonidamine prevented this response (Fig. 4, A and B). Coincident with the basal increase in HK2 (Fig. 1, E and F), higher lactate levels were observed in IPF versus normal lung fibroblasts (Fig. 4C). To further define the metabolic response to profibrotic TGF-β signaling, the OCR was determined by Seahorse analysis (Fig. 4, D and E). Subsequent to measuring the basal OCR, oligomycin [an adenosine triphosphate (ATP) synthase complex V inhibitor that inhibits mitochondrial ATP production], carbonyl cyanide *p*-trifluoromethoxyphenylhydrazone (FCCP; a mitochondrial oxidative phosphorylation uncoupler that allows oxygen consumption by complex IV to reach maximum), and rotenone plus antimycin A (inhibits mitochondrial complexes I and III to shut down mitochondrial respiration) were sequentially added to cells, and the OCR was measured at three distinct time points (Fig. 4D) and averaged (Fig. 4E). We found that TGF-β increased basal respiration, respiration caused by ATP production, maximal respiration, and nonmitochondrial respiration, and these effects were inhibited by Lonidamine, indicating that they depended on HK2 activity.

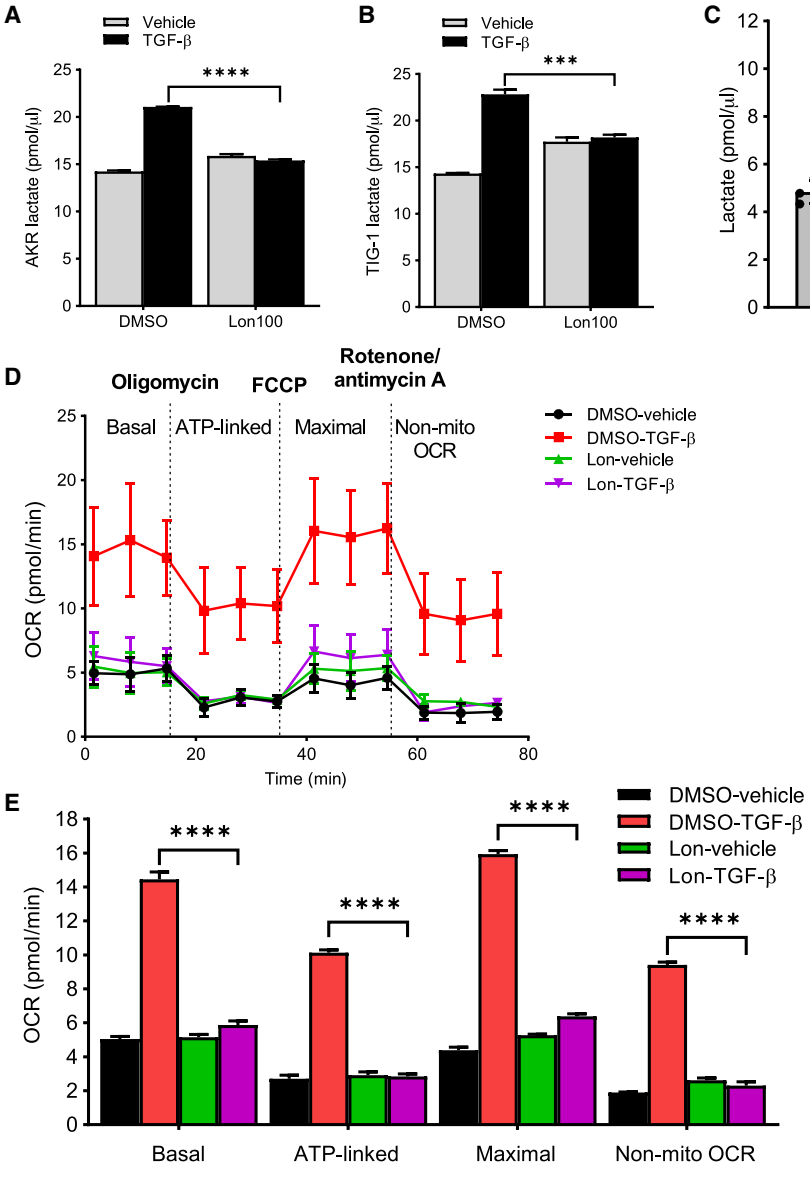

Fig. 4. Lonidamine inhibits TGF-β–stimulated lactate production and oxygen consumption rate. (**A** and **B**) Quiescent AKR-2B (A) and TIG-1 (B) cells were treated for 24 hours with vehicle (DMSO) or Lonidamine in the presence or absence of TGF-β, and intracellular lactate was quantified. $n = 3$ independent experiments. (**C**) Lactate concentration in proliferating human normal lung (NL) and IPF fibroblasts. Data reflect one experiment using patient lung samples from eight normal and seven IPF donors. (**D** and **E**) AKR-2B cells were treated as in (A) and then oxygen consumption rate (OCR) was assessed by the Seahorse XFp Cell Mito Stress Test Kit on a Seahorse XFp extracellular flux analyzer. Data are presented as individual time points (D) and as averages (E). $n = 3$ independent experiments. All data reflect the means ± SEM. Differences between groups were evaluated by two-way ANOVA with Tukey post hoc analysis (A, B, and E) or unpaired Student's *t* test (C). ***$P < 0.001$, ****$P < 0.0001$.

The expression of profibrotic mediators in various disease contexts is often controlled by the transcriptional regulators YAP and TAZ (*44*–*48*). Because TGF-β is a common component critical to the pathogenesis of numerous fibroproliferative disorders and both Smad-dependent and Smad-independent pathways have been implicated in YAP/TAZ activation, we next addressed whether HK2 might stimulate the activity or production of YAP/TAZ downstream of TGF-β signaling. To address that question, we assessed the effect of siRNA-mediated HK2 knockdown on YAP/TAZ-dependent luciferase activity in response to TGF-β treatment in AKR-2B cells. Whereas TGF-β stimulated YAP/TAZ reporter activity ~6-fold, knockdown of HK2 markedly decreased this response (Fig. 5A). We next examined whether the requirement for HK2 in the induction of YAP/TAZ activity by TGF-β was through effects on YAP/TAZ protein abundance. This was examined in both murine (Fig. 5, B and C) and human (Fig. 5, D and E) fibroblasts. HK2 was knocked down with siRNA, and the effect of TGF-β on YAP/TAZ protein levels was examined. Unexpectedly, although TGF-β stimulated TAZ accumulation in an HK2-dependent manner in both murine and human fibroblasts, YAP abundance was unaffected by TGF-β yet similarly dependent on HK2. Consistent with this differential regulation of YAP and TAZ by TGF-β, increased TAZ, but not YAP, was also observed in IPF fibroblasts (Fig. 5, F and G). Although these data place HK2 upstream of YAP/TAZ, other studies in breast cancer have shown that nuclear YAP can modulate HK2 expression (*49*). Therefore, we further assessed the relationship between HK2 and YAP/TAZ and similarly found that endogenous YAP/TAZ was not only downstream of HK2 but that production of endogenous HK2 (but not HK1) required YAP/TAZ (Fig. 5, H and I).

Induction of HK2 is mediated by Smad-dependent and Smad-independent pathways

TGF-β binding to cell membrane receptors activates direct and indirect (*14*, *50*) pathways depending on the cellular context. The canonical Smad pathway is activated within minutes of TGF-β application, whereas activation of other targets such as fatty acid synthase (FASN), ErbB ligands, or mechanistic target of rapamycin (mTOR) requires much longer treatment times (*28*, *51*, *52*). Because HK2 induction occurs relatively late and is maintained throughout 24 hours of TGF-β treatment (Fig. 1), it would not be unexpected for TGF-β to stimulate HK2 accumulation through both canonical and noncanonical mechanisms. Knockdown of Smad2, Smad3, or both Smad2 and Smad3 prevented TGF-β–mediated induction of HK2 (Fig. 6A). Because TGF-β similarly activates a number of signaling pathways resulting in the induction of both ErbB and PDGF ligands (*28*, *51*, *52*), their role in mediating HK2 production was subsequently determined. Whereas pharmacological inhibition of phosphoinositide 3-kinase (PI3K) prevented HK2 production, it was independent of AKT or activation of mTOR complexes 1 and 2

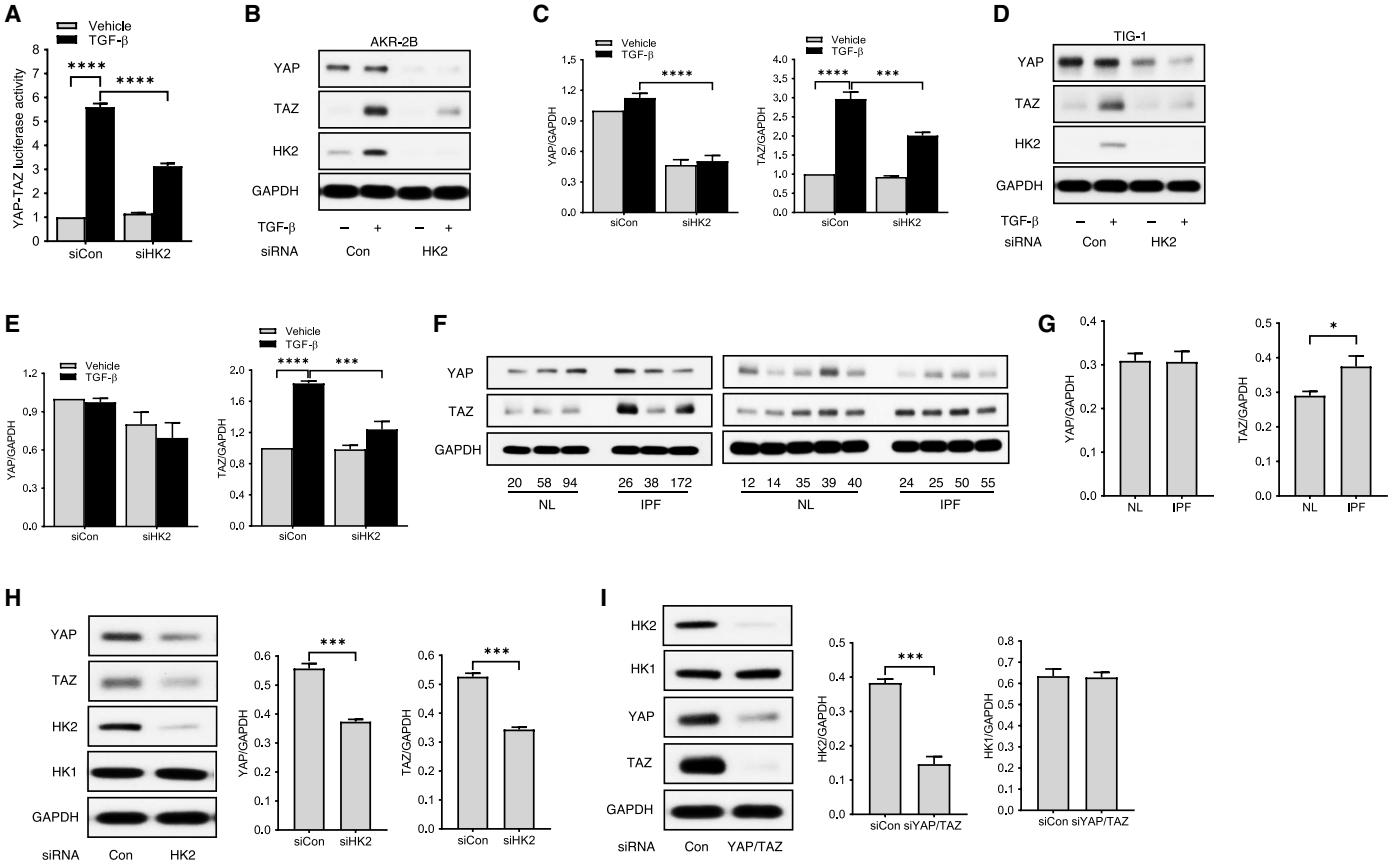

Fig. 5. HK2 mediates the induction of fibrosis by TGF-β through regulation of YAP/TAZ. (**A**) AKR-2B cells were transiently transfected with a YAP/TAZ luciferase reporter and control (siCon) or HK2 (siHK2) siRNA. Luciferase activity was determined after 24 hours in the absence or presence of TGF-β and normalized to the siCon vehicle control. $n = 3$ independent experiments. (**B**) AKR-2B cells were transiently transfected with control or HK2 siRNA, treated for 24 hours with vehicle or TGF-β, and immunoblotted for YAP, TAZ, and HK2. GAPDH is a loading control. Data are representative of three independent experiments. (**C**) Amounts of YAP and TAZ relative to GAPDH in AKR-2B cells treated and analyzed as in (B). $n = 3$ independent experiments. (**D**) Human TIG-1 fibroblasts were treated and immunoblotted as in (B). Data are representative of three independent experiments. (**E**) Amounts of YAP and TAZ relative to GAPDH in TIG-1 cells treated and analyzed as in (D). $n = 3$ independent experiments. (**F**) Immunoblotting for YAP and TAZ in human normal lung (NL) fibroblasts and IPF cells. Numbers indicate cell identifiers. The GAPDH loading control for the samples in the left panel is the same as that in Fig. 1E because the samples were run concurrently on the same gel. (**G**) Amounts of YAP and TAZ relative to GAPDH in normal lung fibroblasts and IPF cells in (F). Data reflect one experiment using patient lung samples from eight normal and seven IPF donors. (**H**) Cycling AKR-2B cells were transiently transfected with control (Con) or HK2 siRNA for 24 hours and Western blotted for YAP, TAZ, HK2, and HK1. Abundances of YAP and TAZ relative to GAPDH are shown. Data are representative of three independent experiments. (**I**) Cycling AKR-2B cells were transfected with control or YAP/TAZ siRNA for 24 hours and Western blotted for the indicated proteins. Abundances of HK2 and HK1 relative to GAPDH are shown. Data are representative of three independent experiments. Differences between groups were evaluated by two-way ANOVA with Tukey post hoc analysis (A, C, and E) or unpaired Student's *t* test (G, H, and I). $^*P < 0.05$, $^{***}P < 0.001$, $^{****}P < 0.0001$.

(mTORC1/2) (Fig. 6B). These findings were further extended by inhibition of MAPK kinase (MEK) with U0126, PDGF signaling with CP673451, or ErbB signaling with lapatinib, which abolished the TGF-β–induced accumulation of HK2 protein (Fig. 6C). Thus, HK2 accumulation was found to depend on Smad2, Smad3, PI3K, MEK, and both PDGF and epidermal growth factor (EGF) signaling stimulated by TGF-β. These pharmacological findings were further confirmed using stable short hairpin RNA (shRNA) knockdown clones for *mTOR*, *Raptor*, *Rictor*, *Erb1/2*, and *PDGFRα/β* (fig. S6, A to C). That HK2 production was modulated by several signaling pathways provides further support to the paradigm that profibrotic TGF-β signaling involves several direct and indirect mediators.

A common downstream mediator of PI3K, MEK, PDGF, and EGF is the transcription factor c-Myc (*53*). To determine whether c-Myc was required for HK2 induction by TGF-β, we stably expressed shRNA targeting *c-Myc* in AKR-2B cells and assessed HK2 protein abundance after TGF-β stimulation using five independent pools of shRNAs targeting distinct sites in *c-Myc*. Whereas knockdown of *c-Myc* prevented the increase in HK2 by TGF-β (Fig. 7A), siRNA-mediated loss of HK2 had no demonstrable effect on the TGF-β induction of c-Myc (Fig. 7, B and C). These findings are consistent with c-Myc being a transcriptional regulator of HK2 (*53*).

Lonidamine inhibition of HK2 activity improves lung function in BLM-induced pulmonary fibrosis

Data from our experiments in fibroblast cell lines and in primary cells from control and patients with IPF demonstrated that HK2 was induced by TGF-β through the integrated actions of both Smad-dependent and Smad-independent pathways, increased in fibroblasts from patients with IPF, and required for the in vitro profibrotic response to TGF-β. We next tested the involvement of HK2 in fibroproliferative disease in vivo. These studies assessed the efficacy of inhibiting HK2

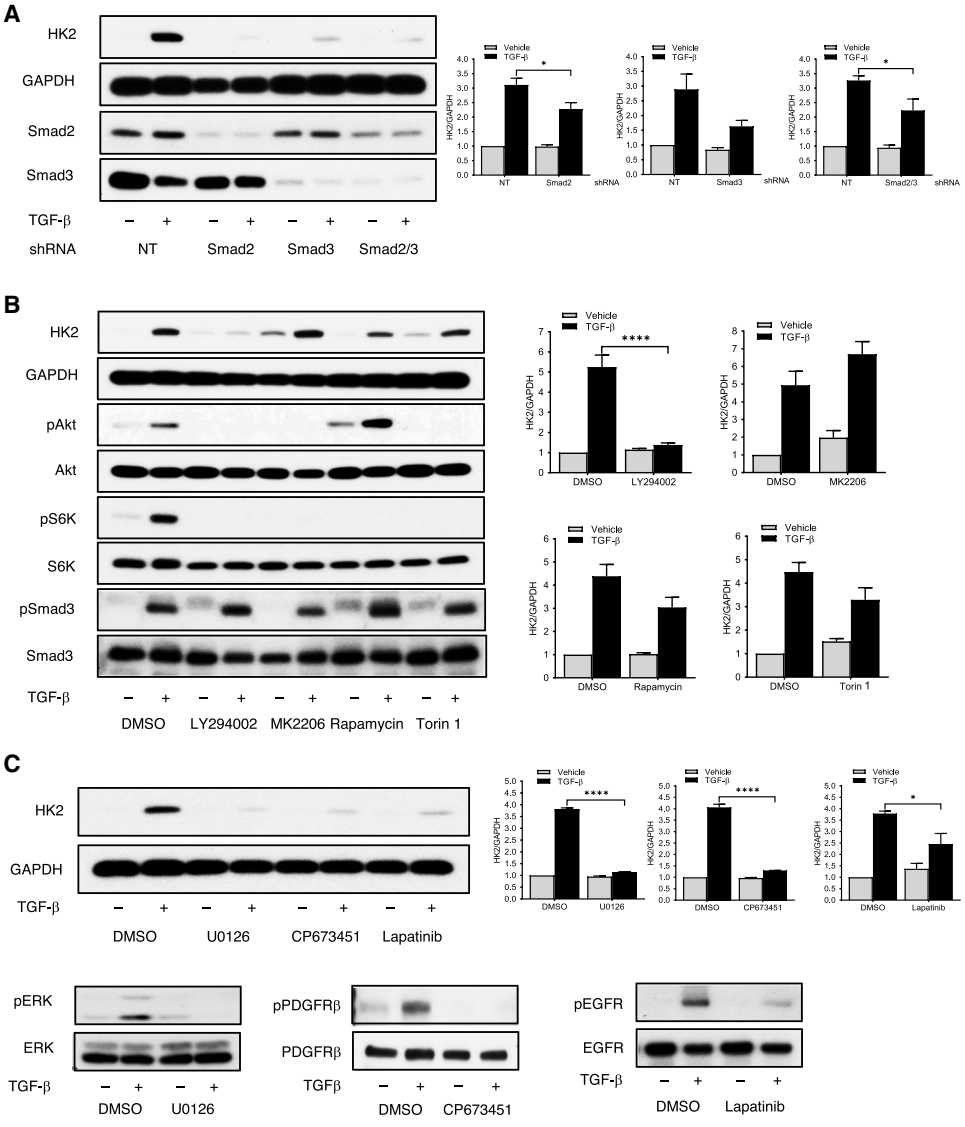

Fig. 6. HK2 induction by TGF-β depends on activation of Smad2/3, PI3K, ERK, PDGFR, and EGFR and is independent of Akt and mTOR. (**A**) AKR-2B cells stably expressing (*35*) nontargeting (NT) shRNA or shRNA targeting Smad2, Smad3, or Smad2 and Smad 3 (Smad2/3) were treated in the absence (–) or presence (+) of TGF-β for 24 hours and Western blotted for HK2, Smad2, and Smad3. GAPDH is a loading control. Amounts of HK2 relative to GAPDH in Smad2, Smad3, or Smad2/3 knockdown cells were determined. $n = 3$ independent experiments. (**B**) AKR-2B cells were stimulated in the absence (–) or presence (+) of TGF-β with vehicle (DMSO), the PI3K inhibitor LY294002, the AKT inhibitor MK2206, the mTORC1 inhibitor rapamycin, or the mTORC1/2 inhibitor Torin 1. Phosphorylated (p) and total Akt, S6 kinase (S6K), and Smad3 were determined 6 hours after stimulation. HK2 and GAPDH were assessed at 24 hours. Amounts of HK2 relative to GAPDH in each treatment group were determined. $n = 3$ independent experiments. (**C**) AKR-2B cells were stimulated in the absence (–) or presence (+) of TGF-β with the indicated compounds vehicle (DMSO), the MEK inhibitor U0126, the PDGFR inhibitor CP673451, or the EGFR inhibitor lapatinib. Abundances of HK2 relative to GAPDH were assessed at 24 hours, pERK/ERK and pPDGFR/PDGFR at 6 hours, and pEGFR/EGFR at 18 hours after simulation. $n = 3$ independent experiments. All data reflect the means ± SEM. Differences between groups were evaluated by two-way ANOVA with Tukey post hoc analysis. $^*P < 0.05$, $^{****}P < 0.0001$.

activity in a murine model of lung fibrosis by starting treatment after the resolution of inflammation and initiation of fibrotic changes (*51*, *54*).

Mice were intratracheally treated with BLM, a common and robust method to induce fibrotic changes in the lung. After BLM challenge, on days 10 to 20, animals were treated daily with either vehicle or the HK2 inhibitor Lonidamine and then euthanized on day 21. To assess lung function throughout the study, peripheral blood oxygenation was determined before and every third or fourth day after the initiation of treatment on day 10. Lonidamine stabilized or improved peripheral blood oxygenation during the course of treatment (Fig. 8A) and reduced collagen deposition in the lung, as assessed by both hydroxyproline content (Fig. 8B) and trichrome staining (Fig. 8Cand fig. S7A). Lonidamine treatment partially or completely reversed the increases in HK2 (Fig. 8D) and lactate (Fig. 8E) induced by BLM and reduced the expression of 10 profibrotic mediators, including transcripts encoding collagen isoforms, EDA-FN, αSMA, and CTGF (Fig. 8F and fig. S7B). FlexiVent analysis indicated that in BLM-treated animals, Lonidamine treatment also improved lung compliance, which describes the ease with which the respiratory system can be extended (fig. S7C). Thus, aspects of normal lung physiology can be restored in BLM-induced pulmonary fibrosis by inhibiting HK2 activity with Lonidamine.

DISCUSSION

Although the relationship between altered metabolism and cellular proliferation has been recognized in the oncologic literature for decades (*55*, *56*), it is only recently that a similar connection has been made between altered cellular metabolism and fibrotic diseases (*35*, *36*, *51*, *57*, *58*). Here, we extend this concept, address the relationship between HK2 and the fibroproliferative activity of TGF-β, and propose a model integrating HK2 into the fibroproliferative processes stimulated by TGF-β (Fig. 9).

Although increased HK2 abundance or activity has been associated with the progression of numerous malignancies (*38*–*40*) and *HK2* transcription is increased by TGF-β and in IPF fibroblasts (*34*), there have been no reports either addressing the underlying mechanism(s) or directly implicating HK2 as a pathogenic mediator or potential therapeutic target for organ fibrosis. This is of particular relevance for diseases such as IPF because, although drugs such as nintedanib and pirfenidone have been approved, disease progression with poor long-term prognosis is still the norm for most patients (*10*, *59*, *60*), and attempts to identify novel therapeutics are ongoing (*61*, *62*). Therefore, we investigated whether HK2 might be a viable target for treating IPF or other fibrotic diseases using both genetic and pharmacological

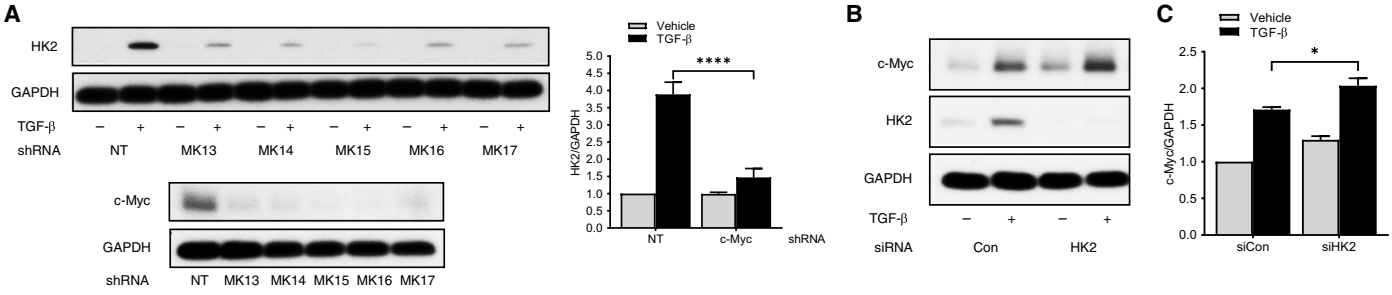

Fig. 7. c-Myc is required for TGF-β–induced accumulation of HK2. (**A**) Quiescent AKR-2B cell lines (MK13 to MK17) stably expressing different shRNAs targeting c-Myc or nontargeting shRNA (shNT) were treated in the absence (–) or presence (+) of TGF-β for 24 hours and Western blotted for HK2. GAPDH is a loading control. Amounts of HK2 in AKR-2B cell lines expressing NT or c-Myc shRNA were determined relative to GAPDH. $n = 5$ cell lines (**B**) AKR-2B cells were transiently transfected with control (siCon) or HK2 (siHK2) siRNA and then stimulated with (+) or without (–) TGF-β for 24 hours. Western blotting was performed for c-Myc, HK2, and GAPDH. Blots are representative of three independent experiments. (**C**) Quantification of c-Myc relative to GAPDH from cells in (B). $n = 3$ independent experiments. All data reflect means ± SEM. Differences between groups were evaluated by two-way ANOVA with Tukey post hoc analysis. *$P < 0.05$, ****$P < 0.0001$.

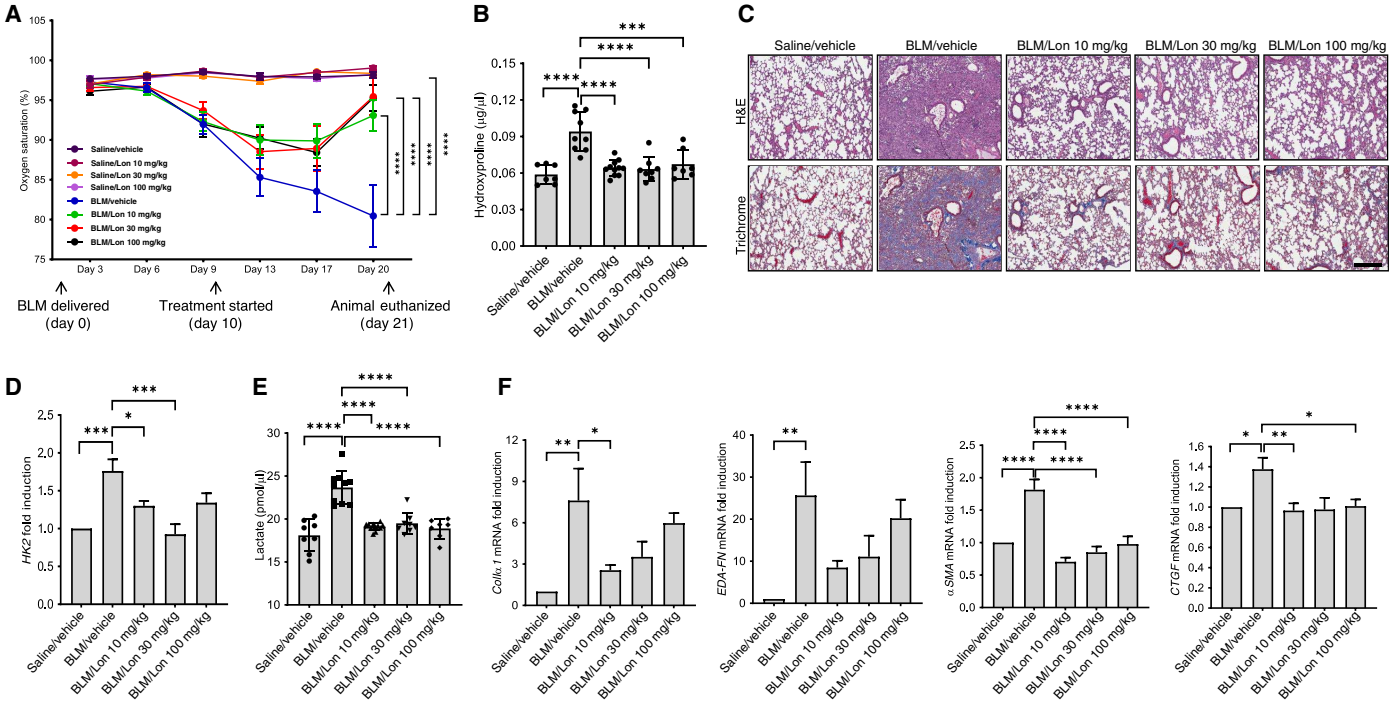

Fig. 8. HK inhibition attenuates bleomycin-induced lung fibrosis. (**A**) C57BL/6 mice were intratracheally treated with saline (control) or bleomycin (BLM) and then treated daily with orally administered vehicle or Lonidamine (Lon) from days 10 to 20 after BLM treatment. Peripheral blood oxygen saturation levels were measured on the days indicated after BLM treatment with room air. (**B**) Total collagen content of lungs from mice treated as in (A) was determined by hydroxyproline assay after euthanasia on day 21. (**C**) Lungs from mice treated as in (A) were analyzed by hematoxylin and eosin (H&E) staining for histology and Masson's trichrome for collagen. Representative images from 7 to 11 mice per treatment group are shown. Scale bar, 300 μm. (**D**) Quantitative PCR for *HK2* in lung tissue from animals treated as indicated and harvested on day 21. (**E**) Total lactate content in lung tissue from animals treated as indicated and harvested on day 21. (**F**) Quantitative PCR for *Col*Iα*1*, *EDA-FN*, α*SMA*, and *CTGF* in lung tissue from animals treated as indicated and harvested on day 21. Data reflect means ± SEM of 7 to 11 mice. Differences between groups were evaluated by one-way ANOVA with Tukey post hoc analysis. *$P < 0.05$, **$P < 0.01$, ***$P < 0.001$, ****$P < 0.0001$.

approaches. TGF-β stimulated HK2, but not HK1, accumulation in various human and mouse fibroblast cell lines and in primary human lung fibroblasts (Fig. 1, A to D, and fig. S1A) (*34*) in a manner that depended on activation of c-Myc through either Smad2/3 or PI3K signaling, or both (Figs. 6, A to C, and 7, A to C). The role of c-Myc in the TGF-β–mediated increase in HK2 is analogous to that reported for the increased glycolysis in nasopharyngeal carcinoma cells by the Epstein-Barr virus latent membrane protein 1 through the stabilization of c-Myc and increased binding of c-Myc to the HK2 promoter (*53*). Consistent with the proliferative activity associated with HK2 expression, fibroblasts from patients with IPF had higher basal abundances of HK2 and lactate (Figs. 1, E and F, and 4C), suggesting that HK2 may have a critical role in maintaining their overall degree of activation.

HK2 was shown to be required for the fibroproliferative actions of TGF-β in vitro (Figs. 2, A to E, and 3, A to F; and figs. S2, A to C, and S5, A to C) and in a murine model of BLM-induced lung fibrosis (Fig. 8, A to F, and fig. S7, A to C). This was assessed by inhibiting

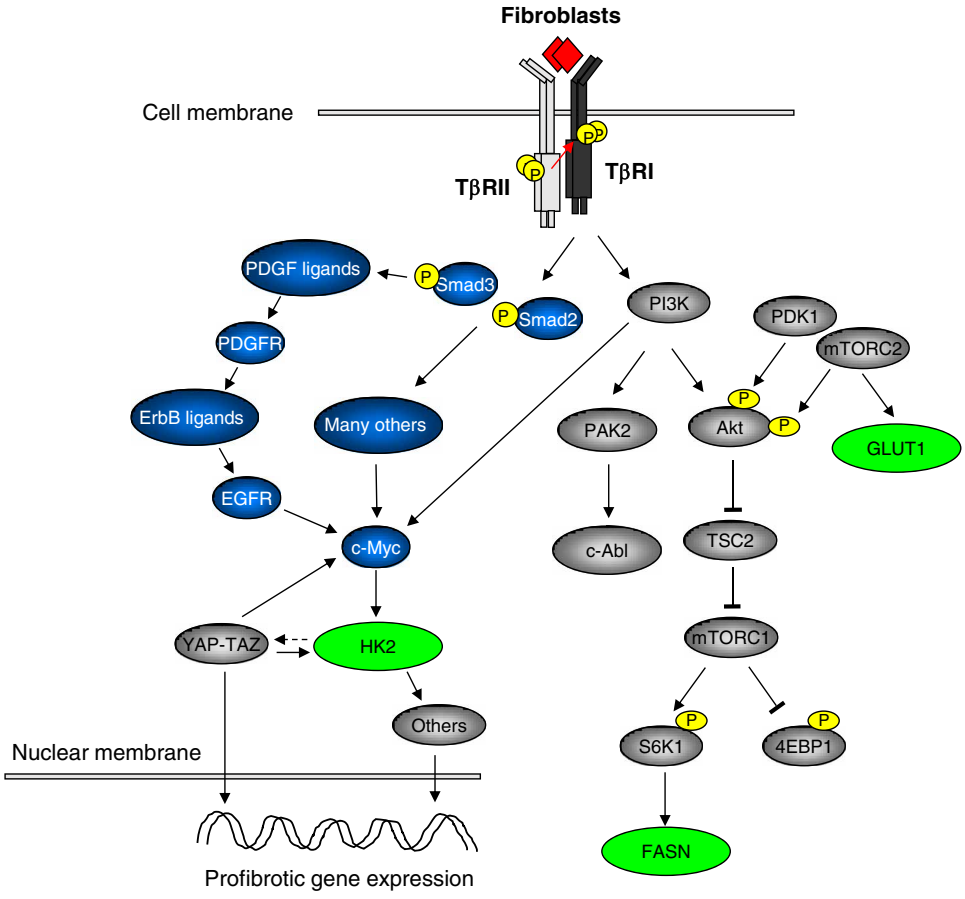

Fig. 9. Proposed model for role of HK2 in profibrotic TGF-β signaling. In fibroblast cells, TGF-β binds to its receptors and activates both canonical (Smad-dependent) and noncanonical pathways. Among these signaling pathways, activation of Smad and/or PI3K signaling leads to the c-Myc–dependent induction of HK2 and subsequent activation of YAP/TAZ through an unknown mechanism. The activity of HK2 contributes to the profibrogenic actions of TGF-β that are mediated by various other mechanisms, some of which are depicted here (*35*, *51*).

HK2 production or activity with siRNA or Lonidamine, respectively. Whereas treatment diminished TGF-β–stimulated cell migration, soft agar colony formation, or induction of profibrotic target genes, this occurred independent of any effect on cell viability or phosphorylation of Smad3 or Akt, canonical and noncanonical mediators of TGF-β signaling, respectively (figs. S3, A and B, and S4, A to E), and was rescued by the exogenous addition of pyruvate to restore oxidative metabolism (Fig. 2C) or overexpression of HK2 (Fig. 3F). It did, however, depend on the kinase activity of HK2 (Fig. 3F) and the transcriptional coactivators YAP and TAZ (Fig. 5, A to I), providing additional evidence for a mechanistic link between glucose metabolism and YAP/TAZ activity (*63*, *64*). Moreover, a direct relationship between YAP/TAZ transcriptional activity and HK-dependent glycolysis has been demonstrated (*65*). YAP/TAZ has long been known as a regulator of development and organ size, and TAZ knockout mice show abnormal alveolarization during lung development, decreased CTGF protein abundance, and resistance to BLM-induced lung fibrosis (*66*). Because YAP/TAZ have also been identified as sensors and mediators of mechanical cues generated by extracellular matrix stiffness or other mechanical forces and can relay the signal into the nucleus to reinforce fibrosis development (*67*, *68*), these functions make YAP/TAZ a good candidate to integrate glycolysis with the development of lung fibrosis. Furthermore, our finding that YAP/TAZ activation was both downstream (Fig. 5, A to H), likely reflecting an indirect role mediated through increased glycolysis, and coincident (Figs. 5I and 9) (*49*) with HK2 documents a complex relationship in need of further investigation. Although HK2 was necessary for basal levels of both YAP and TAZ, only TAZ was increased by TGF-β and showed increased abundance in IPF fibroblasts (Fig. 5, B to G). Analogous differential regulation of YAP/TAZ has been reported in C3H/10T1/2 fibroblasts and experimental kidney fibrosis (*46*).

Although YAP/TAZ are likely to play important roles in linking altered metabolic activity with organ fibrosis, there are likely many other mediators capable of coupling altered HK2 activity with lung fibrosis. For example, it has been shown that increased glycolysis leads to an increase in the tricarboxylic acid cycle intermediate succinate, which stabilizes hypoxia-inducible factor 1-α (HIF-1α) to directly promote myofibroblast differentiation (*34*). HIF-1α could function as another mediator between HK2 and fibrosis development; analogously to YAP/TAZ, HIF-1α also regulates *HK2* expression (*69*). Further study of the relationship between HK2 and HIF-1α could provide additional insight into how glycolysis facilitates lung fibrosis development and expand therapeutic options. Moreover, whereas it has been shown in cancer cells that HK2 can accumulate in the nucleus (*70*), the function of nuclear HK2 is not fully understood. Because myofibroblasts share similar metabolic reprogramming with cancer cells, an intriguing possibility might be that HK2 could also accumulate in the nucleus of IPF cells and affect targets that promote lung fibrosis.

Given that the treatment options for fibroproliferative diseases such as pulmonary fibrosis are limited, we examined the efficacy of Lonidamine inhibition of HK2 activity in the murine BLM model of lung fibrosis using dosages similar to those that have been shown to be effective in tumor studies (*71*–*73*). Not only were various profibrotic target genes and HK2-dependent pathways inhibited by Lonidamine treatment (Fig. 8, B to F, and fig. S7, A and B), but lung function, as assessed by peripheral blood oxygenation, improved (Fig. 8A), and lung compliance, reflecting the ease in which the respiratory system could be expanded, trended upward (fig. S7C). It is noteworthy that optimal in vivo responses were observed at the lower tested doses of Lonidamine. This likely reflects HK2's critical role in cellular physiology and homeostasis. In that Lonidamine inhibits HK1 and HK2, yet abundance of HK1 was not increased by TGF-β or in IPF fibroblasts (Fig. 1, A, E, and F), the development of a selective HK2 inhibitor (*74*) might provide greater efficacy and less toxicity when treatment is systemic. Because the median survival

for patients with IPF is only 2 to 3 years (*75*), identification and characterization of the various operative and interdependent pathways are critical to the creation of effective therapeutic strategies for IPF and other fibrotic disorders. For example, a combinatorial approach targeting HK2, fatty acid synthase (*51*), and/or glutaminase (*76*) might provide greater efficacy because cells can compensate through other pathways if only one enzyme is inhibited. Furthermore, this might be coupled with a nintedanib or pirfenidone rotation to avoid toxic side effects and disease compensation.

MATERIALS AND METHODS

Cell culture

All cells were cultured in medium supplemented with 10% fetal bovine serum (FBS) (HyClone Laboratories) and penicillin-streptomycin (P/S; Life Technologies) at 37°C in 5% CO_2. Murine AKR-2B and Swiss3T3 were cultured in high-glucose DMEM (Dulbecco's modified Eagle's medium) (Life Technologies); human MRC5, IMR90, and TIG-1 cells used Eagle's minimum essential medium (EMEM) (American Type Culture Collection); and 293FT cells used to generate lentiviruses for knockdown of c-*Myc* were cultured in DMEM supplemented with glutamine, sodium pyruvate (Corning Inc.), nonessential amino acids (Corning Inc.), P/S, and G418 (Mediatech). Primary normal human lung fibroblasts were purchased from Lonza and cultured in 10% FBS/EMEM. De-identified primary human normal lung fibroblasts and IPF fibroblasts were obtained from C. Feghali-Bostwick, Medical University South Carolina, Charleston, SC [University of Pittsburgh Institutional Review Board (IRB) no. 970946] and N. Sandbo, University of Wisconsin-Madison, Madison, WI [Translational Science Biocore (TSB) BioBank IRB no. 2011-0521] and characterized in previously published studies (*77*, *78*). They were cultured in 10% FBS/DMEM supplemented with glutamine (cells from C. Feghali-Bostwick; Life Technologies) or no additional additives (cells from N. Sandbo). AKR-2B–derived cell lines stably expressing shRNA for different target genes were cultured in DMEM supplemented with 10% FBS, P/S, and puromycin (1.5 μg/ml; Sigma-Aldrich). The pharmacological inhibitors used are listed in table S1.

Western blotting

Unless stated otherwise, cells were seeded into six-well plates for 24 hours (murine fibroblasts at 5×10^5 cells per well; human fibroblasts at 7×10^5 cells per well) and changed into medium with 0.1% FBS (murine fibroblasts) or without FBS (human fibroblast cells) for 24 hours, and reagents were added for the indicated times. Cellular lysates were prepared on ice with modified radioimmunoprecipitation assay (RIPA) buffer [50 mM tris (pH 7.4), 1% Triton X-100, 0.25% sodium deoxycholate, 150 mM NaCl, 1 mM EDTA (pH 8), and 10 mM NaF] containing cOmplete Protease Inhibitor (Roche). After removal of insoluble material (centrifugation at 16,200*g* at 4°C for 15 min), proteins were separated by electrophoresis on 10% SDS–polyacrylamide gel electrophoresis and processed for Western analysis. Detection was performed using enhanced chemiluminesence (Thermo Fisher Scientific). Commercial antibodies are provided in table S2. Rabbit anti-pSmad3 antibody was used at 1:5000 dilution and generated to the peptide COOH-GSPSIRCSpSVpS (*79*).

Measurement of HK activity

For specific TGF-β (R&D Systems)–induced HK2 activity, 2×10^6 AKR-2B cells were seeded into p100 plates in 10% FBS/DMEM for 24 hours. The medium was changed to 0.1% FBS/DMEM for 24 hours after which cells were pretreated with either dimethyl sulfoxide (DMSO) (0.1%) or SB431542 for 1 hour and then stimulated with either vehicle [4 mM HCl/0.1% bovine serum albumin (BSA)] or TGF-β (10 ng/ml) for 24 hours. Cultures were lysed in modified NP40 RIPA buffer [50 mM tris-HCl (pH 7.4), 150 mM NaCl, 0.25% Na-deoxycholate, 1% IGEPAL CA-630, 1 mM EDTA, 50 mM NaF, and complete protease inhibitor cocktail], and 1 mg of total protein and 0.05 μg of HK2 antibody (Thermo Fisher Scientific) were applied to a Catch-and-Release column (Millipore) as instructed by the manufacturer. Proteins were eluted after addition of 70 μl of nondenaturing elution buffer, and HK2 activity was detected using an HK activity kit (ScienCell Research Laboratories).

For general HK activity detection, 2×10^5 AKR-2B cells were seeded into 12-well plates in 10% FBS/DMEM for 24 hours. The medium was changed to 0.1% FBS/DMEM, and cells were then treated with either DMSO (0.1%) or Lonidamine (25, 50, or 100 μM) (Bio-Techne) for 12 hours. HK activity was determined as above.

Quantitative polymerase chain reaction analysis

Total RNA was isolated from cells or lung tissue using the RNeasy Plus Mini Kit (Qiagen), and 2 μg was reverse-transcribed with random primers (Life Technologies) and Maxima Reverse Transcriptase (Thermo Fisher Scientific) in a 50-μl reaction. The resulting complementary DNA (1 to 5 ng) was used for real-time polymerase chain reaction (PCR) using SYBR Premix Ex Taq II (Takara/Clontech) in a 7500 Fast Real-Time PCR System (Applied Biosystems). *Smad4* was used as a normalization control, and relative expression levels were determined by the $2^{-\Delta\Delta Ct}$ method (*80*). Murine gene primer sets are listed in table S3. All experiments were performed in triplicate.

To extract RNA from mouse lung, tissue was lysed and homogenized with Buffer RLT Plus (supplied with the RNeasy Plus Mini Kit; Qiagen). The lysate was passed through a genomic DNA eliminator spin column, ethanol was added, and the sample was applied to an RNeasy MinElute spin column according to the manufacturer's instructions.

Knockdown by siRNA and shRNA

AKR-2B (2.5×10^5 cells per well) or TIG-1 (5×10^5 cells per well) cells seeded in six-well plates were transiently transfected with 185 pmol siRNA to control (sc-37007), HK2 (sc-35621 or sc-35622), or YAP and TAZ (sc-38638 or sc-38569) (Santa Cruz Biotechnology). Each siRNA contains a pool of three target-specific siRNAs for murine or human cells. Briefly, culture medium was changed to Opti-MEM (Life Technologies) before addition of a mixture of Lipofectamine 2000 (Life Technologies) and siRNA for 6 hours at 37°C. The medium was removed, and cultures were allowed to recover for 18 hours in 10% FBS/DMEM before addition of reagents for the indicated times in low-serum medium (0.1% FBS/DMEM or EMEM).

Plasmids (pLKO.2-puro) encoding shRNA that targeted distinct sites in murine *c-Myc* were purchased from the Mayo Clinic Jacksonville RNA Interference Shared Resource. Production of lentivirus and transduction of AKR-2B cells were performed as previously described (*28*). Stable pools were generated in the presence of puromycin (1.5 μg/ml). shRNA knockdown of *Erb1/2*, *PDGFRα/β*, *mTOR*, *Raptor*, and *Rictor* in AKR-2B cells was described previously (*28*, *50*).

Scratch assay

For scratch assays, 3×10^5 AKR-2B cells were seeded into six-well plates in 10% FBS/DMEM. The next day, the monolayer was disrupted

with a sterile 200-μl pipette tip, and cells were washed with 0.1% FBS/DMEM. Cultures were then treated with the indicated reagents and incubated in the presence or absence of TGF-β (5 ng/ml) for 24 hours at 37°C. Images (×100) were taken at 24 hours, and the cellular leading edge was measured and quantified.

Soft agar/anchorage-independent growth

Soft agar assays were performed as previously described (*28*). Briefly, 1.25×10^4 cells were plated in six-well plates in the presence or absence of TGF-β (25 ng/ml) ± Lonidamine or the indicated siRNA at 37°C. After 7 days of growth at 37°C, the number of colonies ≥50 μm in diameter was counted using an Optronix Gelcount (Oxford Optronix). All experiments were performed in triplicate.

Lactate assay

AKR-2B (5×10^5 per well) and TIG-1 (7×10^5 per well) cells were seeded in six-well plates for 24 hours. After 24 hours of serum starvation (0.1% FBS/DMEM AKR-2B; serum-free EMEM TIG-1), cells were then pretreated with DMSO (0.1%) or Lonidamine (100 μM) at 37°C for 1 hour followed by vehicle or TGF-β (10 ng/ml) for 24 hours and homogenized in Lactate Assay Buffer (BioVision). Cycling normal lung and IPF fibroblast cells were harvested in Lactate Assay Buffer, which was also used to homogenize mouse lung tissue. Lactate levels were determined using 10 μg of protein (all cells and tissues) with the PicoProbe Lactate Fluorometric Assay Kit (BioVision) and measured with a multimode reader (BioTek).

Seahorse assay

AKR-2B cells were plated and treated essentially as described in lactate assay. After 24 hours of starvation, cultures were then suspended in 0.1% FBS/DMEM containing the indicated treatment(s), and 3000 cells were seeded into Seahorse assay microplates (Agilent Technologies). After 24 hours of incubation, the medium was changed to Seahorse XF base assay medium supplemented with 1 mM sodium pyruvate, 2 mM L-glutamine, and 10 mM glucose for 1 hour at 37°C in a non-CO_2 incubator. OCR was measured on a Seahorse XFp extracellular flux analyzer by using the Seahorse XFp Cell Mito Stress Test Kit (Agilent Technologies) under basal conditions and in response to 1 μM oligomycin, 0.5 μM FCCP, and 0.5 μM rotenone and antimycin A.

Luciferase reporter assays

To determine luciferase activity, 2.5×10^5 AKR-2B cells were transfected with 2 μg of a YAP/TAZ luciferase reporter plasmid (8xGTIIC-luciferase; a gift from S. Piccolo, Addgene plasmid no. 34615) (Addgene) (*67*), 0.5 μg of cytomegalovirus-β-galactosidase, and 110 pmol siRNA (control or HK2). Twenty-four hours after transfection, the medium was changed to 0.1% FBS/DMEM either with vehicle (4 mM HCl/0.1% BSA) or with TGF-β for 24 hours. Cells were washed with phosphate-buffered saline (PBS) and harvested in reporter lysis buffer (Promega). Luciferase activity was determined in a Lumat 9507 luminometer (Berthold Technologies) after normalization for transfection efficiency by detecting β-galactosidase activity with chlorophenol red-β-D-galactopyranoside and measuring substrate conversion at 562 nm.

MTT and Fluor cell viability determination

For MTT assays, 2.5×10^3 AKR-2B cells were seeded into 96-well plates with 10% FBS/DMEM. After 24 hours of incubation, cultures were treated with the indicated concentrations of Lonidamine in 0.1% FBS/DMEM in a total volume of 100 μl for 24 hours. Ten microliters of MTT/PBS (5 mg/ml; Sigma-Aldrich) was then added to the culture medium, and after 4 hours of incubation, 100 μl of DMSO was added for 10 min at room temperature. Color reaction was read at 570 nm.

Cell integrity was determined on 2×10^4 AKR-2B cells seeded into 96-well culture plates with black wall and lid (Greiner Bio-One) in 100 μl of 10% FBS/DMEM. After 24 hours of incubation, cultures were treated with the indicated reagents in 0.1% FBS/DMEM in a total volume of 100 μl for 24 hours. CellTiter-Fluor Reagent (Promega) was added for 1.5 hours at 22 hours of treatment as instructed by the manufacturer, and fluorescence was read with excitation wavelength at 370 nm and emission wavelength at 505 nm.

Rescue HK2 inhibition

AKR-2B cells were transfected with siCon or siHK2 using Lipofectamine 2000 for 24 hours. After addition of either water (vehicle) or 5 mM sodium pyruvate (Sigma-Aldrich) for 1 hour, cultures were stimulated with vehicle or TGF-β (10 ng/ml) for 24 hours at 37°C in 0.1% FBS/DMEM. Cultures were then processed for Western blotting.

To determine whether wild-type or kinase dead HK2 could overcome the inhibitory actions of Lonidamine, cultures were transfected as above with 5 μg of control (pEGFP-N1), kinase active HK2 (pGFPN3-HK2WT), or kinase-impaired HK2 (pGFPN3-HK2mut) (gifts from H. Ardehali, Addgene plasmid nos. 21920 and 21922) (Addgene) (*81*). Cultures were then pretreated with either DMSO (0.1%) or Lonidamine (75 μM) for 1 hour, followed by 24 hours of stimulation with vehicle or TGF-β (10 ng/ml) in 0.1% FBS/DMEM. Cells were then lysed with RIPA buffer and processed for Western blotting.

Immunofluorescence (mitochondrial) staining

MRC5 cells (1×10^5) were seeded onto coverslips in six-well plates in 10% FBS/EMEM for 24 hours. Cultures were changed to 0.1% FBS/EMEM and treated with either vehicle (4 mM HCl/0.1% BSA) or TGF-β (5 ng/ml) for a total of 6 hours, with MitoTracker (200 nM; Invitrogen) added for the last 30 min. Cultures were then fixed with 3% paraformaldehyde, permeabilized with 0.1% Triton X-100, blocked with 0.1% BSA/10% normal goat serum/PBS, and incubated overnight with HK2 antibody at 4°C. After washing with PBS, HK2 was labeled with 488-Goat-anti-rabbit secondary antibody (Life Technologies) at room temperature for 2 hours, whereas nuclei were stained with 4′,6-diamidino-2-phenylindole at room temperature for 5 min. Fluorescence images were collected on an LSM510 confocal microscope (Carl Zeiss Microimage Inc.). Percentage of colocalization of HK2 with MitoTracker was analyzed by ImageJ software (National Institutes of Health).

BLM model of lung fibrosis

All procedures involving animals were approved by and performed according to the guidelines of the Mayo Clinic Institutional Animal Care and Use Committee (A615-15). C57BL/6 mice (12 weeks, females), on breeder chow and water ad libitum, were treated with 50 μl of 0.9% saline or BLM (2 U/kg; Mayo Clinic Pharmacy) by tracheal instillation using an intratracheal aerosolizer (Penn-Century). Gavage (200 μl) with vehicle (1% carboxymethylcellulose sodium) or the indicated concentration (10, 30, or 100 mg/kg) of the HK inhibitor Lonidamine (Selleckchem) was initiated on day 10 after BLM instillation and repeated every day for 11 days. Peripheral blood oxygen levels (on room air) were measured using a MouseOX collar clip

monitoring system (Starr Life Science) on days 3, 6, 9, 13, 16, and 20 after BLM instillation. Animals were maintained on a 12-hour light/dark cycle, and all interventions were performed during the animal's light cycle. On day 21, all mice were euthanized by pentobarbital (Mayo Clinic Pharmacy) injection, FlexiVent was performed, and lungs were excised, weighed, and prepared for histologic and other analyses.

Hydroxyproline determination

Total lung collagen levels were assessed using the Hydroxyproline Assay Kit (Sigma-Aldrich). Briefly, mouse lung tissue samples were homogenized with H_2O to a concentration of 100 mg/ml. Samples (100 μl) were hydrolyzed by the addition of 100 μl of 12 M HCl, and duplicate 5-μl aliquots were analyzed according to the manufacturer's instructions.

Statistical analysis

Statistical analyses were performed by using GraphPad Prism 8.1 software. Differences between two groups were evaluated by unpaired Student's *t* test or among groups by one-way analysis of variance (ANOVA) with Tukey post hoc test or two-way ANOVA with Tukey post hoc analysis.

SUPPLEMENTARY MATERIALS

stke.sciencemag.org/cgi/content/full/12/612/eaax4067/DC1

Fig. S1. Quantitation of TGF-β–induced HK2 accumulation in murine and human fibroblasts and mitochondrial translocation of HK2.

Fig. S2. Quantitation of profibrotic proteins in AKR-2B and TIG-1 cells after HK2 knockdown.

Fig. S3. HK2 knockdown does not affect TGF-β–induced activation of Smad3 or Akt.

Fig. S4. Effect of Lonidamine on HK activity, production, cell viability, and TGF-β signaling.

Fig. S5. Quantitation of profibrotic TGF-β targets in AKR-2B and TIG-1 cells treated with Lonidamine.

Fig. S6. TGF-β–induced HK2 production is mediated by EGFR and PDGFR but not the mTOR pathway.

Fig. S7. HK inhibition improves lung structure, total collagen content, profibrotic gene expression, and tissue compliance in BLM-induced lung fibrosis.

Table S1. Pharmacological inhibitors.

Table S2. Commercial antibodies.

Table S3. Quantitative PCR murine primers.

View/request a protocol for this paper from *Bio-protocol*.

REFERENCES AND NOTES

1. A. Leask, Potential therapeutic targets for cardiac fibrosis: TGFβ, angiotensin, endothelin, CCN2, and PDGF, partners in fibroblast activation. *Circ. Res.* **106**, 1675–1680 (2010).
2. M. P. Steele, D. A. Schwartz, Molecular mechanisms in progressive idiopathic pulmonary fibrosis. *Annu. Rev. Med.* **64**, 265–276 (2013).
3. R. Weiskirchen, S. Weiskirchen, F. Tacke, Organ and tissue fibrosis: Molecular signals, cellular mechanisms and translational implications. *Mol. Aspects Med.* **65**, 2–15 (2019).
4. T. A. Wynn, T. R. Ramalingam, Mechanisms of fibrosis: Therapeutic translation for fibrotic disease. *Nat. Med.* **18**, 1028–1040 (2012).
5. P. Sivakumar, P. Ntolios, G. Jenkins, G. Laurent, Into the matrix: Targeting fibroblasts in pulmonary fibrosis. *Curr. Opin. Pulm. Med.* **18**, 462–469 (2012).
6. T. A. Wynn, Common and unique mechanisms regulate fibrosis in various fibroproliferative diseases. *J. Clin. Invest.* **117**, 524–529 (2007).
7. M. Zeisberg, R. Kalluri, Cellular mechanisms of tissue fibrosis. 1. Common and organ-specific mechanisms associated with tissue fibrosis. *Am. J. Physiol. Cell Physiol.* **304**, C216–C225 (2013).
8. C. Beyer, O. Distler, J. H. Distler, Innovative antifibrotic therapies in systemic sclerosis. *Curr. Opin. Rheumatol.* **24**, 274–280 (2012).
9. J. Rosenbloom, S. V. Castro, S. A. Jimenez, Narrative review: Fibrotic diseases: Cellular and molecular mechanisms and novel therapies. *Ann. Intern. Med.* **152**, 159–166 (2010).
10. W. J. Canestaro, S. H. Forrester, G. Raghu, L. Ho, B. E. Devine, Drug treatment of idiopathic pulmonary fibrosis: Systematic review and network meta-analysis. *Chest* **149**, 756–766 (2016).
11. H. E. Jo, S. Randhawa, T. J. Corte, Y. Moodley, Idiopathic pulmonary fibrosis and the elderly: Diagnosis and management considerations. *Drugs Aging* **33**, 321–334 (2016).
12. Y. Li, H. Xu, W. Wu, J. Ye, D. Fang, D. Shi, L. Li, Clinical application of angiotensin receptor blockers in patients with non-alcoholic fatty liver disease: A systematic review and meta-analysis. *Oncotarget* **9**, 24155–24167 (2018).
13. H. Loomis-King, K. R. Flaherty, B. B. Moore, Pathogenesis, current treatments and future directions for idiopathic pulmonary fibrosis. *Curr. Opin. Pharmacol.* **13**, 377–385 (2013).
14. E. B. Leof, J. A. Proper, A. S. Goustin, G. D. Shipley, P. E. DiCorleto, H. L. Moses, Induction of c-sis mRNA and activity similar to platelet-derived growth factor by transforming growth factor beta: A proposed model for indirect mitogenesis involving autocrine activity. *Proc. Natl. Acad. Sci. U.S.A.* **83**, 2453–2457 (1986).
15. M. Andrianifahanana, M. C. Wilkes, C. E. Repellin, M. Edens, T. J. Kottom, R. A. Rahimi, E. B. Leof, ERBB receptor activation is required for profibrotic responses to transforming growth factor β. *Cancer Res.* **70**, 7421–7430 (2010).
16. E. J. Battegay, E. W. Raines, R. A. Seifert, D. F. Bowen-Pope, R. Ross, TGF-β induces bimodal proliferation of connective tissue cells via complex control of an autocrine PDGF loop. *Cell* **63**, 515–524 (1990).
17. S. Colak, P. Ten Dijke, Targeting TGF-beta signaling in cancer. *Trends Cancer* **3**, 56–71 (2017).
18. C. J. David, J. Massagué, Contextual determinants of TGFβ action in development, immunity and cancer. *Nat. Rev. Mol. Cell Biol.* **19**, 419–435 (2018).
19. E. H. Budi, J. Xu, R. Derynck, Regulation of TGF-β receptors. *Methods Mol. Biol.* **1344**, 1–33 (2016).
20. C. H. Bassing, J. M. Yingling, D. J. Howe, T. Wang, W. W. He, M. L. Gustafson, P. Shah, P. K. Donahoe, X.-F. Wang, A transforming growth factor b type I receptor that signals to activate gene expression. *Science* **263**, 87–89 (1994).
21. H. Y. Lin, X. F. Wang, E. E. Ng, R. A. Weinberg, H. F. Lodish, Expression cloning of the TGF-beta type II receptor, a functional transmembrane serine/threonine kinase. *Cell* **68**, 775–785 (1992).
22. R. A. Anders, E. B. Leof, Chimeric granulocyte/macrophage colony-stimulating factor/transforming growth factor-β (TGF-β) receptors define a model system for investigating the role of homomeric and heteromeric receptors in TGF-ß signaling. *J. Biol. Chem.* **271**, 21758–21766 (1996).
23. J. L. Wrana, L. Attisano, R. Wieser, F. Ventura, J. Massagué, Mechanism of activation of the TGF-β receptor. *Nature* **370**, 341–347 (1994).
24. E. H. Budi, D. Duan, R. Derynck, Transforming growth factor-β receptors and Smads: Regulatory complexity and functional versatility. *Trends Cell Biol.* **27**, 658–672 (2017).
25. C. S. Hill, Transcriptional control by the SMADs. *Cold Spring Harb. Perspect. Biol.* **8**, a022079 (2016).
26. B. A. Hocevar, T. L. Brown, P. H. Howe, TGF-beta induces fibronectin synthesis through a c-Jun N-terminal kinase-dependent, Smad4-independent pathway. *EMBO J.* **18**, 1345–1356 (1999).
27. A. Moustakas, C. H. Heldin, Non-Smad TGF-β signals. *J. Cell Sci.* **118**, 3573–3584 (2005).
28. R. Rahimi, M. Andrianifahanana, M. C. Wilkes, M. E. Edens, T. J. Kottom, J. Blenis, E. B. Leof, Distinct roles for mammalian target of rapamycin complexes in the fibroblast response to transforming growth factor-β. *Cancer Res.* **69**, 84–93 (2009).
29. M. Agathocleous, W. A. Harris, Metabolism in physiological cell proliferation and differentiation. *Trends Cell Biol.* **23**, 484–492 (2013).
30. N. N. Pavlova, C. B. Thompson, The emerging hallmarks of cancer metabolism. *Cell Metab.* **23**, 27–47 (2016).
31. K. Bernard, N. J. Logsdon, G. A. Benavides, Y. Sanders, J. Zhang, V. M. Darley-Usmar, V. J. Thannickal, Glutaminolysis is required for transforming growth factor-β1-induced myofibroblast differentiation and activation. *J. Biol. Chem.* **293**, 1218–1228 (2018).
32. R. M. Kottmann, A. A. Kulkarni, K. A. Smolnycki, E. Lyda, T. Dahanayake, R. Salibi, S. Honnons, C. Jones, N. G. Isern, J. Z. Hu, S. D. Nathan, G. Grant, R. P. Phipps, P. J. Sime, Lactic acid is elevated in idiopathic pulmonary fibrosis and induces myofibroblast differentiation via pH-dependent activation of transforming growth factor-β. *Am. J. Respir. Crit. Care Med.* **186**, 740–751 (2012).
33. S. Rangarajan, N. B. Bone, A. A. Zmijewska, S. Jiang, D. W. Park, K. Bernard, M. L. Locy, S. Ravi, J. Deshane, R. B. Mannon, E. Abraham, V. Darley-Usmar, V. J. Thannickal, J. W. Zmijewski, Metformin reverses established lung fibrosis in a bleomycin model. *Nat. Med.* **24**, 1121–1127 (2018).
34. N. Xie, Z. Tan, S. Banerjee, H. Cui, J. Ge, R.-M. Liu, K. Bernard, V. J. Thannickal, G. Liu, Glycolytic reprogramming in myofibroblast differentiation and lung fibrosis. *Am. J. Respir. Crit. Care Med.* **192**, 1462–1474 (2015).
35. M. Andrianifahanana, D. M. Hernandez, X. Yin, J.-H. Kang, M.-Y. Jung, Y. Wang, E. S. Yi, A. C. Roden, A. H. Limper, E. B. Leof, Profibrotic up-regulation of glucose transporter 1 by TGF-β involves activation of MEK and mammalian target of rapamycin complex 2 pathways. *FASEB J.* **30**, 3733–3744 (2016).
36. B. Selvarajah, I. Azuelos, M. Plate, D. Guillotin, E. J. Forty, G. Contento, H. V. Woodcock, M. Redding, A. Taylor, G. Brunori, P. F. Durrenberger, R. Ronzoni, A. D. Blanchard, P. F. Mercer, D. Anastasiou, R. C. Chambers, mTORC1 amplifies the ATF4-dependent de novo serine-glycine pathway to supply glycine during TGF-β_1-induced collagen biosynthesis. *Sci. Signal.* **12**, eaav3048 (2019).

37. R. B. Robey, N. Hay, Mitochondrial hexokinases: Guardians of the mitochondria. *Cell Cycle* **4**, 654–658 (2005).
38. K. C. Patra, Q. Wang, P. T. Bhaskar, L. Miller, Z. Wang, W. Wheaton, N. Chandel, M. Laakso, W. J. Muller, E. L. Allen, A. K. Jha, G. A. Smolen, M. F. Clasquin, R. B. Robey, N. Hay, Hexokinase 2 is required for tumor initiation and maintenance and its systemic deletion is therapeutic in mouse models of cancer. *Cancer Cell* **24**, 213–228 (2013).
39. D. J. Roberts, V. P. Tan-Sah, E. Y. Ding, J. M. Smith, S. Miyamoto, Hexokinase-II positively regulates glucose starvation-induced autophagy through TORC1 inhibition. *Mol. Cell* **53**, 521–533 (2014).
40. R. B. Robey, N. Hay, Mitochondrial hexokinases, novel mediators of the antiapoptotic effects of growth factors and Akt. *Oncogene* **25**, 4683–4696 (2006).
41. M. K. Phanish, N. A. Wahab, P. Colville-Nash, B. M. Hendry, M. E. Dockrell, The differential role of Smad2 and Smad3 in the regulation of pro-fibrotic TGFβ1 responses in human proximal-tubule epithelial cells. *Biochem. J.* **393**, 601–607 (2006).
42. F. Verrecchia, A. Mauviel, Transforming growth factor-β and fibrosis. *World J. Gastroenterol.* **13**, 3056–3062 (2007).
43. J. Wu, L. Hu, F. Wu, L. Zou, T. He, Poor prognosis of hexokinase 2 overexpression in solid tumors of digestive system: A meta-analysis. *Oncotarget* **8**, 32332–32344 (2017).
44. S. Anorga, J. M. Overstreet, L. L. Falke, J. Tang, R. G. Goldschmeding, P. J. Higgins, R. Samarakoon, Deregulation of Hippo-TAZ pathway during renal injury confers a fibrotic maladaptive phenotype. *FASEB J.* **32**, 2644–2657 (2018).
45. A. J. Jorgenson, K. M. Choi, D. Sicard, K. M. Smith, S. E. Hiemer, X. Varelas, D. J. Tschumperlin, TAZ activation drives fibroblast spheroid growth, expression of profibrotic paracrine signals, and context-dependent ECM gene expression. *Am. J. Physiol. Cell Physiol.* **312**, C277–C285 (2017).
46. M. Z. Miranda, J. F. Bialik, P. Speight, Q. Dan, T. Yeung, K. Szaszi, S. F. Pedersen, A. Kapus, TGF-β1 regulates the expression and transcriptional activity of TAZ protein via a Smad3-independent, myocardin-related transcription factor-mediated mechanism. *J. Biol. Chem.* **292**, 14902–14920 (2017).
47. S. Noguchi, A. Saito, Y. Mikami, H. Urushiyama, M. Horie, H. Matsuzaki, H. Takeshima, K. Makita, N. Miyashita, A. Mitani, T. Jo, Y. Yamauchi, Y. Terasaki, T. Nagase, TAZ contributes to pulmonary fibrosis by activating profibrotic functions of lung fibroblasts. *Sci. Rep.* **7**, 42595 (2017).
48. T. Panciera, L. Azzolin, M. Cordenonsi, S. Piccolo, Mechanobiology of YAP and TAZ in physiology and disease. *Nat. Rev. Mol. Cell Biol.* **18**, 758–770 (2017).
49. Y. Gao, Y. Yang, F. Yuan, J. Huang, W. Xu, B. Mao, Z. Yuan, W. Bi, TNFα-YAP/p65-HK2 axis mediates breast cancer cell migration. *Oncogene* **6**, e383 (2017).
50. M. Andrianifahanana, M. C. Wilkes, S. K. Gupta, R. A. Rahimi, C. E. Repellin, M. Edens, J. Wittenberger, X. Yin, E. Maidl, J. Becker, E. B. Leof, Profibrotic TGFbeta responses require the cooperative action of PDGF and ErbB receptor tyrosine kinases. *FASEB J.* **27**, 4444–4454 (2013).
51. M. Y. Jung, J.-H. Kang, D. M. Hernandez, X. Yin, M. Andrianifahanana, Y. Wang, A. Gonzalez-Guerrico, A. H. Limper, R. Lupu, E. B. Leof, Fatty acid synthase is required for profibrotic TGF-β signaling. *FASEB J.* **32**, 3803–3815 (2018).
52. S. Lamouille, R. Derynck, Cell size and invasion in TGF-β–induced epithelial to mesenchymal transition is regulated by activation of the mTOR pathway. *J. Cell Biol.* **178**, 437–451 (2007).
53. L. Xiao, Z.-y. Hu, X. Dong, Z. Tan, W. Li, M. Tang, L. Chen, L. Yang, Y. Tao, Y. Jiang, J. Li, B. Yi, B. Li, S. Fan, S. You, X. Deng, F. Hu, L. Feng, A. M. Bode, Z. Dong, L. Q. Sun, Y. Cao, Targeting Epstein-Barr virus oncoprotein LMP1-mediated glycolysis sensitizes nasopharyngeal carcinoma to radiation therapy. *Oncogene* **33**, 4568–4578 (2014).
54. N. I. Chaudhary, A. Schnapp, J. E. Park, Pharmacologic differentiation of inflammation and fibrosis in the rat bleomycin model. *Am. J. Respir. Crit. Care Med.* **173**, 769–776 (2006).
55. P. Icard, L. Fournel, Z. Wu, M. Alifano, H. Lincet, Interconnection between metabolism and cell cycle in cancer. *Trends Biochem. Sci.* (2019).
56. O. Warburg, On respiratory impairment in cancer cells. *Science* **124**, 269–270 (1956).
57. K. Bernard, N. J. Logsdon, S. Ravi, N. Xie, B. P. Persons, S. Rangarajan, J. W. Zmijewski, K. Mitra, G. Liu, V. M. Darley-Usmar, V. J. Thannickal, Metabolic reprogramming is required for myofibroblast contractility and differentiation. *J. Biol. Chem.* **290**, 25427–25438 (2015).
58. Y. P. Kang, S. B. Lee, J.-m. Lee, H. M. Kim, J. Y. Hong, W. J. Lee, C. W. Choi, H. K. Shin, D.-j. Kim, E. S. Koh, C.-S. Park, S.-W. Kwon, S. W. Park, Metabolic profiling regarding pathogenesis of idiopathic pulmonary fibrosis. *J. Proteome Res.* **15**, 1717–1724 (2016).
59. T. E. King Jr., W. Z. Bradford, S. Castro-Bernardini, E. A. Fagan, I. Glaspole, M. K. Glassberg, E. Gorina, P. M. Hopkins, D. Kardatzke, L. Lancaster, D. J. Lederer, S. D. Nathan, C. A. Pereira, S. A. Sahn, R. Sussman, J. J. Swigris, P. W. Noble; ASCEND Study Group, A phase 3 trial of pirfenidone in patients with idiopathic pulmonary fibrosis. *N. Engl. J. Med.* **370**, 2083–2092 (2014).
60. L. Richeldi, R. M. du Bois, G. Raghu, A. Azuma, K. K. Brown, U. Costabel, V. Cottin, K. R. Flaherty, D. M. Hansell, Y. Inoue, D. S. Kim, M. Kolb, A. G. Nicholson, P. W. Noble, M. Selman, H. Taniguchi, M. Brun, F. Le Maulf, M. Girard, S. Stowasser, R. Schlenker-Herceg, B. Disse, H. R. Collard; INPULSIS Trial Investigators, Efficacy and safety of nintedanib in idiopathic pulmonary fibrosis. *N. Engl. J. Med.* **370**, 2071–2082 (2014).
61. D. J. Lederer, F. J. Martinez, Idiopathic pulmonary fibrosis. *N. Engl. J. Med.* **378**, 1811–1823 (2018).
62. A. L. Mora, M. Rojas, A. Pardo, M. Selman, Emerging therapies for idiopathic pulmonary fibrosis, a progressive age-related disease. *Nat. Rev. Drug Discov.* **16**, 810 (2017).
63. J.-S. Mo, Z. Meng, Y. C. Kim, H. W. Park, C. G. Hansen, S. Kim, D.-S. Lim, K.-L. Guan, Cellular energy stress induces AMPK-mediated regulation of YAP and the Hippo pathway. *Nat. Cell Biol.* **17**, 500–510 (2015).
64. W. Wang, Z.-D. Xiao, X. Li, K. E. Aziz, B. Gan, R. L. Johnson, J. Chen, AMPK modulates Hippo pathway activity to regulate energy homeostasis. *Nat. Cell Biol.* **17**, 490–499 (2015).
65. E. Enzo, G. Santinon, A. Pocaterra, M. Aragona, S. Bresolin, M. Forcato, D. Grifoni, A. Pession, F. Zanconato, G. Guzzo, S. Bicciato, S. Dupont, Aerobic glycolysis tunes YAP/TAZ transcriptional activity. *EMBO J.* **34**, 1349–1370 (2015).
66. A. Mitani, T. Nagase, K. Fukuchi, H. Aburatani, R. Makita, H. Kurihara, Transcriptional coactivator with PDZ-binding motif is essential for normal alveolarization in mice. *Am. J. Respir. Crit. Care Med.* **180**, 326–338 (2009).
67. S. Dupont, L. Morsut, M. Aragona, E. Enzo, S. Giulitti, M. Cordenonsi, F. Zanconato, J. Le Digabel, M. Forcato, S. Bicciato, N. Elvassore, S. Piccolo, Role of YAP/TAZ in mechanotransduction. *Nature* **474**, 179–183 (2011).
68. F. Liu, D. Lagares, K. M. Choi, L. Stopfer, A. Marinkovic, V. Vrbanac, C. K. Probst, S. E. Hiemer, T. H. Sisson, J. C. Horowitz, I. O. Rosas, L. E. Fredenburgh, C. Feghali-Bostwick, X. Varelas, A. M. Tager, D. J. Tschumperlin, Mechanosignaling through YAP and TAZ drives fibroblast activation and fibrosis. *Am. J. Physiol. Lung Cell. Mol. Physiol.* **308**, L344–L357 (2015).
69. G. N. Masoud, W. Li, HIF-1α pathway: Role, regulation and intervention for cancer therapy. *Acta Pharm. Sin. B* **5**, 378–389 (2015).
70. C. L. Neary, J. G. Pastorino, Nucleocytoplasmic shuttling of hexokinase II in a cancer cell. *Biochem. Biophys. Res. Commun.* **394**, 1075–1081 (2010).
71. D. Cervantes-Madrid, G. Dominguez-Gomez, A. Gonzalez-Fierro, E. Perez-Cardenas, L. Taja-Chayeb, C. Trejo-Becerril, A. Duenas-Gonzalez, Feasibility and antitumor efficacy in vivo, of simultaneously targeting glycolysis, glutaminolysis and fatty acid synthesis using lonidamine, 6-diazo-5-oxo-L-norleucine and orlistat in colon cancer. *Oncol. Lett.* **13**, 1905–1910 (2017).
72. K. Nath, D. S. Nelson, D. F. Heitjan, D. B. Leeper, R. Zhou, J. D. Glickson, Lonidamine induces intracellular tumor acidification and ATP depletion in breast, prostate and ovarian cancer xenografts and potentiates response to doxorubicin. *NMR Biomed.* **28**, 281–290 (2015).
73. K. Nath, D. S. Nelson, J. Roman, M. E. Putt, S. C. Lee, D. B. Leeper, J. D. Glickson, Effect of lonidamine on systemic therapy of DB-1 human melanoma xenografts with temozolomide. *Anticancer Res* **37**, 3413–3421 (2017).
74. S. N. Garcia, R. C. Guedes, M. M. Marques, Unlocking the potential of HK2 in cancer metabolism and therapeutics. *Curr. Med. Chem.* 10.2174/0929867326666181213092652 , (2018).
75. G. Raghu, H. R. Collard, J. J. Egan, F. J. Martinez, J. Behr, K. K. Brown, T. V. Colby, J. F. Cordier, K. R. Flaherty, J. A. Lasky, D. A. Lynch, J. H. Ryu, J. J. Swigris, A. U. Wells, J. Ancochea, D. Bouros, C. Carvalho, U. Costabel, M. Ebina, D. M. Hansell, T. Johkoh, D. S. Kim, T. E. King Jr., Y. Kondoh, J. Myers, N. L. Muller, A. G. Nicholson, L. Richeldi, M. Selman, R. F. Dudden, B. S. Griss, S. L. Protzko, H. J. Schünemann; ATS/ERS/JRS/ALAT Committee on Idiopathic Pulmonary Fibrosis, An official ATS/ERS/JRS/ALAT statement: Idiopathic pulmonary fibrosis: Evidence-based guidelines for diagnosis and management. *Am. J. Respir. Crit. Care Med.* **183**, 788–824 (2011).
76. H. Cui, N. Xie, D. Jiang, S. Banerjee, J. Ge, Y. Y. Sanders, G. Liu, Inhibition of glutaminase 1 attenuates experimental pulmonary fibrosis. *Am. J. Respir. Cell Mol. Biol.* **61**, 492–500 (2019).
77. S. Esnault, E. E. Torr, K. Bernau, M. W. Johansson, E. A. Kelly, N. Sandbo, N. N. Jarjour, Endogenous semaphorin-7A impedes human lung fibroblast differentiation. *PLOS ONE* **12**, e0170207 (2017).
78. J. M. Pilewski, L. Liu, A. C. Henry, A. V. Knauer, C. A. Feghali-Bostwick, Insulin-like growth factor binding proteins 3 and 5 are overexpressed in idiopathic pulmonary fibrosis and contribute to extracellular matrix deposition. *Am. J. Pathol.* **166**, 399–407 (2005).
79. M. C. Wilkes, S. J. Murphy, N. Garamszegi, E. B. Leof, Cell-type-specific activation of PAK2 by transforming growth factor ß independent of Smad2 and Smad3. *Mol. Cell. Biol.* **23**, 8878–8889 (2003).
80. K. J. Livak, T. D. Schmittgen, Analysis of relative gene expression data using real-time quantitative PCR and the $2^{-\Delta\Delta C}_T$ method. *Methods* **25**, 402–408 (2001).
81. L. Sun, S. Shukair, T. J. Naik, F. Moazed, H. Ardehali, Glucose phosphorylation and mitochondrial binding are required for the protective effects of hexokinases I and II. *Mol. Cell. Biol.* **28**, 1007–1017 (2008).

Acknowledgments: We thank N. Hay, University of Illinois at Chicago, for helpful discussions in the initiation of the study and A. Kanakkanthara for substantial assistance in the Seahorse analysis. Primary fibroblasts from normal donors and patients with IPF were provided by C. Feghali-Bostwick, Medical University of South Carolina, and N. Sandbo, University of Wisconsin-Madison. **Funding:** This work was supported by Public Health Service Grants GM-54200 and GM-55816 from the National Institute of General Medical Sciences, the Caerus Foundation (91736058), and the Mayo Foundation (to E.B.L.). **Author contributions:** X.Y. and E.B.L. designed

the research and wrote the paper. X.Y., M.C., J.-H.K., K.J.S., M.-Y.J., M.A., and D.M.H. performed research, with the majority done by X.Y. All authors analyzed the data and revised the paper. **Competing interests:** The authors declare that they have no competing interests. **Data and materials availability:** All data needed to evaluate the conclusions in the paper are present in the paper or the Supplementary Materials. A material transfer agreement (MTA) between the University of Padua and the Mayo Clinic exists for plasmid 34615 (8xGTIIC-luciferase) provided by S. Piccolo. An MTA between Northwestern University and the Mayo Clinic exists for plasmids 21920 (FLHKII-pGFPN3) and 21922 (MuHKII-pGFPN3) provided by H. Ardehali.

Submitted 20 March 2019
Accepted 22 November 2019
Published 17 December 2019
10.1126/scisignal.aax4067

Citation: X. Yin, M. Choudhury, J.-H. Kang, K. J. Schaefbauer, M.-Y. Jung, M. Andrianifahanana, D. M. Hernandez, E. B. Leof, Hexokinase 2 couples glycolysis with the profibrotic actions of TGF-β. *Sci. Signal.* **12**, eaax4067 (2019).

Science Signaling

Hexokinase 2 couples glycolysis with the profibrotic actions of TGF-β

Xueqian Yin, Malay Choudhury, Jeong-Han Kang, Kyle J. Schaefbauer, Mi-Yeon Jung, Mahefatiana Andrianifahanana, Danielle M. Hernandez and Edward B. Leof

Sci. Signal. **12** (612), eaax4067.
DOI: 10.1126/scisignal.aax4067

Glycolysis promotes lung fibrosis

Transforming growth factor–β (TGF-β) promotes fibrosis by stimulating fibroblasts to proliferate and differentiate into matrix-secreting myofibroblasts. Yin *et al.* found that the glycolytic enzyme hexokinase 2 (HK2) was highly abundant in lung fibroblasts from patients with idiopathic pulmonary fibrosis (IPF) and that TGF- β induced the accumulation of HK2 and stimulated glycolysis in mouse and human lung fibroblasts. Pharmacological inhibition of HK2 with Lonidamine attenuated the profibrotic actions of TGF-β in fibroblasts. Lonidamine also reduced molecular markers of fibrosis and improved lung function in a mouse model of lung fibrosis. Thus, HK2-dependent metabolic dysregulation contributes to lung fibrosis and is a potential therapeutic target.